ATOMS MADE ENTIRELY OF ANTIMATTER: TWO METHODS PRODUCE SLOW ANTIHYDROGEN

G. GABRIELSE

Harvard University, Cambridge MA 02138, USA

I. Introduction and Overview 156
II. Motivations 162
A. Testing CPT Invariance 162
B. Extensions to the Standard Model that Violate Lorentz Invariance 166
C. Antihydrogen Gravity Tests 166
III. Ingredients of Slow Antihydrogen 168
A. Cold Antiprotons for All Slow $\overline{H}$ Experiments 168
B. A New Storage Ring for Antihydrogen Experiments 170
C. Better Efficiency with More Deceleration 170
D. Five Methods to Accumulate Cold Positrons 171
E. Plasma Diagnostics 173
IV. Production Method I: During e^+ Cooling of $\overline{p}$ in a Nested Penning Trap 175
A. Nested Penning Trap and Positron Cooling of Antiprotons 175
B. Demonstration and Study of Positron Cooling of Antiprotons 176
C. A Variation: Driven e^+ Cooling of $\overline{p}$ 180
D. Antiproton Losses from a Nested Penning Trap 182
E. Two Techniques to Count $\overline{H}$ Atoms 182
V. Beyond Counting $\overline{H}$ Atoms 185
A. Probing Internal $\overline{H}$ Orbits 185
B. Measured Field Ionization Spectrum 186
C. Beyond Guiding Center Atoms 190
D. First Measurement of the Speed of Slow $\overline{H}$ Atoms 191
E. Deexcitation of Highly Excited States 194
VI. Three Body $\overline{H}$ Formation, and Related Experiments 195
VII. Production Method II: Laser-Controlled $\overline{H}$ Production 198
VIII. Comparing the $\overline{H}$ Production Methods 200
IX. Future 200
A. AntihydrogenTrapping 200
B. Will Collisions with Matter Atoms Cool or Annihilate $\overline{H}$ Atoms? 205
C. Continuous Lyman Alpha Source 207
X. Conclusions 208
XI. Acknowledgments 210
XII. References 210

1049-250X DOI: 10.1016/S1049-250X(04)50004-6

An antihydrogen ($\overline{H}$) atom – a positron (e^+) in orbit about an antiproton ($\overline{p}$) – is the simplest atom made entirely of antimatter. Producing $\overline{H}$ atoms that are cold enough to be trapped for precise laser spectroscopy, to compare antihydrogen and hydrogen, is a goal that has been pursued for many years. A prequel to this review summarized the techniques for accumulating cold $\overline{p}$ and e^+ that opened the way to slow $\overline{H}$ production, along with crucial devices like the nested Penning trap that was developed to bring the $\overline{p}$ and e^+ together. Several exciting years have seen the first production, observations and studies of slow $\overline{H}$ atoms – so far by two different methods. The demonstration of e^+ cooling of $\overline{p}$ in a nested Penning trap led to observations of slow $\overline{H}$ atoms produced in this way (method I) using two detection techniques. Field ionization detection of $\overline{H}$ produced by method I makes it possible to go beyond the simple counting of $\overline{H}$ atoms – to probe their internal structure and measure their velocity. The atoms identified so far are thus shown to be in highly excited states and to be traveling much too rapidly to trap. The new techniques to probe the internal state and speed are the necessary first steps towards developing methods to attain ground state $\overline{H}$ atoms that are much colder. In a very different method II, lasers control the production of $\overline{H}$ atoms via charge exchange collisions – a method that seems to naturally produce $\overline{H}$ atoms with essentially the low energy distribution of the $\overline{p}$ from which they form.

I. Introduction and Overview

Antihydrogen ($\overline{H}$), the simplest of antimatter atoms, is the bound state of a positron (e^+) in orbit around an antiproton ($\overline{p}$). Are the properties of this atom made entirely of antimatter precisely the same as those of hydrogen, its matter counterpart, as CPT invariance would indicate (Sect. II)? Is there any difference between the gravitational acceleration of a matter and an antimatter atom? How dow we produce these atoms in order to look for answers to these questions?

An 1986 Erice lecture (Gabrielse, 1987), shortly after $\overline{p}$ were trapped for the first time (Gabrielse *et al.*, 1986a), laid out the antihydrogen goals that are now being pursued by three international collaborations at the CERN Antiproton Decelerator (AD) – a unique storage ring built to conduct these studies.

> "For me, the most attractive way ... would be to capture the antihydrogen in a neutral particle trap ... The objective would be to then study the properties of a small number of [antihydrogen] atoms confined in the neutral trap for a long time."

Inspiration came from attempts to confine neutrons (Kügler *et al.*, 1978) and the first trapping of atoms (Migdall *et al.*, 1985). The trap first used for atoms would not allow the bias field that we needed to simultaneously trap $\bar{p}$ and e^+, but the use of a Ioffe trap (Gott *et al.*, 1962) had been proposed for confining atoms in a nearly uniform bias field (Pritchard, 1983).

Trapping of cold $\overline{H}$ still seems like the most feasible way to make optimal use of $\overline{H}$ atoms for precise measurements, since the number of $\overline{H}$ that will be produced still seems likely to be orders of magnitude less than typically used for hydrogen experiments. Trapping of charged particles and ions for precise measurements was already familiar in 1986, and atom trapping has since become just as common. A proposal to trap hydrogen as a way to produce Bose–Einstein condensates was reported about the same time as the Erice lecture (Hess, 1986), and hydrogen trapping is also now common (Hess *et al.*, 1987; Roijen *et al.*, 1988; Setija *et al.*, 1993; Cesar *et al.*, 1996). If the accuracy now achieved in the spectroscopy of hydrogen (Niering *et al.*, 2000) could be realized with antihydrogen, a lepton and baryon CPT test of unprecedented accuracy would be possible. Gravitational studies of $\overline{H}$ seem very difficult but are not excluded in principle (Gabrielse, 1988; Walz and Hänsch, 2004).

Some years later, while we were developing and demonstrating the techniques needed to make low energy $\overline{H}$ atoms, suggestions were made (Baur, 1993; Munger *et al.*, 1993; Munger *et al.*, 1994) to form very rapidly moving $\overline{H}$ by arranging that $\bar{p}$ in a storage ring pick up e^+ from pair production (Aste, 1994; Bertulani and Baur, 1998). This led to the first production and observation of $\overline{H}$ atoms. First, the 9 atoms observed at CERN were reported (Baur *et al.*, 1996), and then 37 atoms were observed at Fermilab (Blanford *et al.*, 1998). There was considerable interest in these observations both in the scientific community and beyond.

Nonetheless, producing cold antihydrogen still seemed like the most feasible way to produce antihydrogen atoms that could be precisely compared to hydrogen atoms. Cold $\bar{p}$ and cold e^+ are essential ingredients (Sect. III). The prequel to this review, entitled "Comparing the Antiproton and Proton, and Opening the Way to Cold Antihydrogen" (Gabrielse, 2001), tells the 15-year story of developing the $\bar{p}$ techniques that now make all slow $\overline{H}$ experiments possible. Our TRAP Collaboration slowed (Gabrielse *et al.*, 1989a), trapped (Gabrielse *et al.*, 1986b), electron-cooled (Gabrielse *et al.*, 1989b), and accumulated 4 K $\bar{p}$ (Gabrielse *et al.*, 1990) at an energy 10^{10} times lower in energy than had been previously realized (Sect. III). They were then used to compare the charge-to-mass ratios of antiproton and proton to an accuracy that was nearly a million times better than had been previously achieved. Antiproton stacking techniques (Gabrielse, 2001) are now the only way to obtain large numbers of cold $\bar{p}$ at

the AD (Gabrielse *et al.*, 2002c). If all of these $\bar{p}$ techniques are applied after the $\bar{p}$ from the AD are first slowed in a decelerator, then it seems likely that many more $\bar{p}$ will be captured and transferred to an experiment trap. Cold e^+, the other essential ingredients of cold antihydrogen, are also briefly discussed.

This review contains an exciting update. Just several years later, slow antihydrogen atoms are now being regularly produced by two different methods:

(1) $\overline{H}$ production in a nested Penning trap (Gabrielse *et al.*, 1988) during positron cooling of antiprotons (Gabrielse *et al.*, 2001) (Sect. IV).
(2) Laser-controlled $\overline{H}$ production, in which lasers select the $\overline{H}$ binding energy (Storry *et al.*, 2004) (Sect. VII).

Our ATRAP Collaboration (table I) developed method I over many years (Gabrielse *et al.*, 1988; Hall and Gabrielse, 1996; Gabrielse *et al.*, 1999a, 2001) and method II much more recently (Hessels *et al.*, 1998; Speck *et al.*, 2004; Storry *et al.*, 2004). Two different detection methods have been used (Sect. IV.E). ATRAP uses background-free, field ionization detection to count the $\overline{H}$ produced by both method I (Gabrielse *et al.*, 2002a,b) and method II (Storry *et al.*, 2004). The ATHENA Collaboration produces $\overline{H}$ using method I, counting an $\overline{H}$ atom upon detecting the correlated loss of a e^+ and a $\bar{p}$ taking place within 5 μs and ±8 mm of each other (M. Amoretti *et al.*, 2002). Both collaborations count large numbers of $\overline{H}$ atoms.

Table I
ATRAP collaboration: CERN AD-2.

Harvard University: Prof. G. Gabrielse[1], Dr. C.H. Storry, Dr. J.N. Tan, N.S. Bowden, J. Estrada, N. Guise, P. Larochelle, D. LeSage, P. Oxley, A. Speck, M. Wessels, P. Yesley

Institute for Atomic and Molecular Physics FOM, Amsterdam: C. Wesdorp

IKP, Forschungszentrum Jülich: Prof. W. Oelert, Dr. F. Goldenbaum, Dr. D. Grzonka, Dr. S. Martin, Dr. G. Schepers, Dr. T. Sefzick

Max-Planck-Institut für Quantenoptik, Garching: H. Pittner, J. Walz, T.W. Hänsch[2]

Vrije Universiteit, Amsterdam: Dr. K.S.E. Eikema

York University: Prof. E.A. Hessels, D. Comeau

Early contributions came from the Univ. of Bonn, and from the Inst. for Med. En. Phys. in Vienna.

*Spokesperson. [1]Also Ludwig-Maximilians-Universität München.

ATRAP's field ionization detection technique (Gabrielse *et al.*, 2002b) makes it possible to go beyond counting $\overline{H}$ atoms (Sect. V) – revealing that it is highly excited $\overline{H}$ that are produced in large numbers (Gabrielse *et al.*, 2004a), and that so far these are moving too rapidly to be trapped (Gabrielse *et al.*, 2004b). The central challenge facing $\overline{H}$ research right now is in obtaining $\overline{H}$ atoms that are useful for precise spectroscopy, with at least the following two properties:

(1) Useful $\overline{H}$ must be in its ground state.
(2) Useful $\overline{H}$ must be moving slowly enough to be trapped, with energy much less than the 0.5 K depth of the deepest magnetic traps.

Field ionization detection probes the internal $\overline{H}$ state by determining which $\overline{H}$ are deeply enough bound to survive an analyzing electric field. Recent theory provides the relationship between the size of the atoms produced and the electric field that they can survive (Vrinceanu *et al.*, 2004). The $\overline{H}$ velocity is probed by making the strength of the analyzing electric field oscillate in time. The number of $\overline{H}$ that survive this field depends upon the $\overline{H}$ velocity (Gabrielse *et al.*, 2004b) since faster atoms travel through the oscillating field without ionizing during the time that this field has a low magnitude. The ATRAP measurement of $\overline{H}$ velocity demonstrated for the first time that $\overline{H}$ formation is faster than e^+ cooling, so that $\overline{H}$ can be formed before the $\bar{p}$ and e^+ come into thermal equilibrium. No useful $\overline{H}$ has yet been identified. However, the new techniques to probe the $\overline{H}$ state and velocity should enable $\overline{H}$ production to be optimized for the production of the most tightly bound states, and for the lowest $\overline{H}$ velocity.

Almost all observed $\overline{H}$ atoms have so far been produced using method I – during positron cooling of antiprotons in a nested Penning trap (Fig. 1) – rather than in the more recently demonstrated method II. The highly excited $\overline{H}$ states that are being produced at a high rate, revealed by field ionization detection (Gabrielse *et al.*, 2002b, 2004a), are what was expected for $\overline{H}$ formation at low temperatures using finite-sized plasmas of e^+ and $\bar{p}$. Many years ago we pointed out that the expected high rate $\overline{H}$ production mechanism at low temperatures T should be the three body formation process (Sect. VI) whose rate varies as $T^{-9/2}$(Gabrielse *et al.*, 1988)

$$\bar{p} + e^+ + e^+ \longrightarrow \overline{H}^* + e^+. \qquad (1)$$

The matter counterpart of this process had been studied for the much higher temperatures of interest for astrophysical applications (Bates *et al.*, 1962; Makin and Keck, 1963; Stevefelt *et al.*, 1975). It was exciting to realize that the production rate could be enormous if we did the experiments

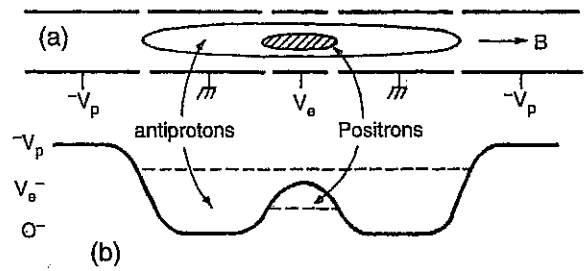

FIG. 1. Outline (a) and potentials (b) of a nested Penning trap used to produce positrons cooling of antiprotons, and the accompanying production slow $\overline{H}$. Variations of this figure, taken from the original proposal (Gabrielse *et al.*, 1988), are now familiar in papers on slow antihydrogen since most slow $\overline{H}$ has been produced in this way.

at much lower temperatures – provided that the steep temperature scaling was valid down to much lower T than had been previously considered, and provided that the strong magnetic field used to confine the $\bar{p}$ and e^+ did not reduce the rate too badly. The questions raised about temperature scaling and the effect of fields triggered theoretical work that suggested that the temperature scaling would be valid both without (Zygelman and Dalgarno, 1989; Zygelman, 2003) and with (Glinsky and O'Neil, 1991; Men'shikov and Fedichev, 1995; Fedichev, 1997) a strong magnetic field. The strong field only decreased the high formation rate by a factor of ten (Glinsky and O'Neil, 1991) or even somewhat less (Robicheaux and Hanson, 2004). For a $\bar{p}$ in an infinitely extended plasma, ground state $\overline{H}$ would be the expected eventual outcome. However, it was immediately clear that for the limited interaction time of a $\bar{p}$ within the finite size plasmas that can be arranged in an ion trap, the three body formation would be "interrupted" when the $\overline{H}^*$ left the e^+ plasma. $\overline{H}$ atoms in the highest excited states would be ionized by the trap fields, but the interrupted three body formation could then result in highly excited $\overline{H}^*$ produced at a high rate, just as is now observed, and the theoretical work thus sought to determine the time scale.

Can low temperature $\overline{H}$ be produced by $\overline{H}$ production method I? It is too early to tell. The most straight-forward positron cooling of antiprotons (used by ATRAP for its initial $\overline{H}$ observation and by ATHENA for all of its $\overline{H}$ studies) could form $\overline{H}$ with an appreciable velocity if the $\overline{H}$ forms before the e^+ have completely cooled the $\bar{p}$. However, ATRAP almost immediately moved to a variation on method I – driving the $\overline{H}$ production through repeated cycles of e^+ cooling of $\bar{p}$ (Gabrielse *et al.*, 2002b). This variation produces $\overline{H}$ more efficiently, and should also make it possible to give the $\bar{p}$ just the minimum velocity needed to produce $\overline{H}$. The needed optimization of the drive was not done for the initial demonstration of measuring an

$\overline{H}$ velocity, so it remains to be seen if the low velocities hoped for can be realized. The weak dependence of the $\overline{H}$ formation rate upon the temperature of heated e^+ plasmas measured by ATHENA (Amoretti, *et al.*, 2004) (contrary to what was expected for three body formation) was interpreted as if the $\bar{p}$ and e^+ were in thermal equilibrium. Likely it instead indicates rapid three body formation of very fast $\overline{H}$ – relatively independent of the equilibrium e^+ temperature, an interpretation born out of a very recent simulation (Robicheaux, 2004).

The first laser-controlled $\overline{H}$ production (method II) was demonstrated only very recently (Speck *et al.*, 2004; Storry *et al.*, 2004),

$$h\nu(852\text{ nm}) + h\nu(511\text{ nm}) + Cs \longrightarrow Cs^* \tag{2}$$

$$Cs^* + e^+ \longrightarrow Ps^* + Cs^+ \tag{3}$$

$$Ps^* + \bar{p} \longrightarrow \overline{H}^* + e^-, \tag{4}$$

Field ionization detection reveals that highly excited $\overline{H}^*$ is also being formed by this process, as expected for resonant charge exchange collisions (Hessels *et al.*, 1998). An attractive feature is that the $\overline{H}$ produced seems likely to have the energy distribution of the $\bar{p}$ from which it forms, though this remains to be confirmed experimentally. Although the $\bar{p}$ temperature can be no lower than the ambient 4 K temperature in the initial proof-of-principle experiment (Storry *et al.*, 2004), the $\bar{p}$ temperature could be made much lower in principle, by adapting techniques which took a trapped electron to 300 mK (D'Urso *et al.*, 2003), for example. The only calculation of laser-controlled $\overline{H}$ production is for no magnetic field (Hessels *et al.*, 1998), so formation theory that includes a strong magnetic field is clearly needed.

Other possible formation methods have been discussed. ATRAP was unable to get another promising $\overline{H}$ production mechanism – field-assisted formation (Wesdorp *et al.*, 2000) – to work for reasons that are not completely clear. Another attractive possibility, suggested long ago, is to use a CO_2 laser to stimulate trapped $\bar{p}$ and e^+ to form $\overline{H}$ $n \approx 10$ states (Gabrielse *et al.*, 1988), which would then rapidly deexcite to the ground state by radiation. There may be an enhancement (Wolf, 1993) if the photon energy is tuned lower by several kT to take advantage of a deexcitation "bottleneck" predicted by a more recent theory (Glinsky and O'Neil, 1991).

Some progress has been made on topics that will be important for future experiments (Sect. IX). We find it attractive to superimpose a neutral particle trap for $\overline{H}$, in the same volume within which Penning traps contain the $\bar{p}$ and e^+ ingredients (Squires *et al.*, 2001) from which $\overline{H}$ atoms

form (Sect. IX.A). The challenge (Sect. IX.A) arises for magnetic gradient traps that destroy the cylindrical symmetry, and hence angular momentum conservation, thereby voiding a confinement theorem (O'Neil, 1980) which prevents radial diffusion of the charged ingredients from their traps. Many recent calculations investigate the feasibility of cooling $\overline{H}$ atoms in collisions with matter atoms (Sect. IX.B). In an important step on the way to the first $\overline{H}$ spectroscopy, a continuous Lyman alpha radiation source (Eikema *et al.*, 1999) has been used for hydrogen 1s–2p spectroscopy (Eikema *et al.*, 2001), a demonstration that bodes well for the $\overline{H}$ future.

Space does not permit discussing two related topics that should at least be mentioned. The first is the possibility to directly measure the $\bar{p}$ magnetic moment, building on techniques we developed to measure the magnetic moment of the free electron (D'Urso *et al.*, 2004), and also on a double trap developed to measure the magnetic moment of an electron bound to an ion (Verdú *et al.*, 2003). The second is the discovery of a small polarization correction to the cyclotron frequency of a molecular ion (Thompson *et al.*, 2004). When applied to the q/m comparison of the antiproton and proton (which uses an H^-ion) (Gabrielse *et al.*, 1999b), this shift slightly within its error bars the precise comparison of q/m for the antiproton and proton (Gabrielse, 2004; Thompson *et al.*, 2004) that was summarized in the prequel to this work (Gabrielse, 2001).

A conclusion (Sect. X) expresses optimism for the future, but readily admits that much remains to be done.

II. Motivations

A. Testing CPT Invariance

The "P" in CPT stands for a parity transformation. Suppose we perform a certain experiment and measure a certain outcome. As we do the experiment, we also watch what the experiment and outcome look like in a mirror (actually the reflection describe and a rotation by 180 degrees that we will ignore). We then build an apparatus and carry out a second experiment which is identical to the mirror image of the first. If reality is invariant under parity transformations P then we should obtain the outcome seen in the mirror for the second experiment. Until 1956 it was believed that reality was invariant under parity transformations. Then Lee and Yang noticed that this basic tenet of physicists' faith had not been tested for weak interactions, those interactions between particles which are responsible for radioactive decay of nuclei. Shortly after, Wu and collaborators, and then several other experimental groups in rapid succession, showed in fact

that experiments and mirror image experiments produced strikingly different results when weak interactions were involved. The widespread faith that reality was invariant under parity transformations P had clearly been misplaced.

A new faith, that reality is invariant under CP transformations, rapidly replaced the discredited notion. The "C" stands for a charge conjugation transformation, which for our purposes is a transformation in which particles are turned into their antiparticles. To test whether reality is invariant under CP transformations, a mirror image experiment is constructed as above but this time all the particles within it are also changed into antiparticles. It was widely believed that these two different experiments could not be distinguished by their outcomes until Cronin and Fitch surprised everyone by using kaon particles to explicitly demonstrate that our reality is not invariant under CP transformations. The experiment has been repeated by different groups in different locations and related measurements are still being pursued.

Now most physicists believe that reality is instead invariant under CPT transformations, the "T" standing for time reversal transformations. CPT invariance seems more well-founded insofar as theorists find it virtually impossible to construct a reasonable theory which violates this invariance. Axiomatic quantum field theory, for example, used commonly to describe all interactions except for gravity, is CPT invariant. To experimentally test for CPT invariance, one again compares the outcomes of two experiments. This time one makes a movie of the goings on in a mirror image experiment in which the particles are switched to antiparticles. The second experiment is constructed to mimic what one sees in the movie when the movie is run backwards (i.e., when "time is reversed").

In practice, the cyclotron oscillation frequencies of a proton and an antiproton oscillating in the same magnetic field would be identical if reality is invariant under CPT transformations. Our antiproton-proton frequency comparison reviewed in the prequel to this paper (Gabrielse, 2001) is by far the most precise test of CPT invariance done with baryons and antibaryons, particles made of three quark particles or three antiquark particles. The antiproton-to-proton charge-to-mass ratio comparison thus joins an experiment with kaons (made of a quark particle and an antiquark particle) and a lepton comparison of the magnetic moments of an electron and positron as one of the most precise experimental tests of whether our reality is invariant under CPT transformations.

The various tests of CPT made by comparing the measured properties of particles and antiparticles are represented in Fig. 2. The stable particles and antiparticles in these tests come in several varieties which are important to distinguish. The proton (antiproton) is a baryon (antibaryon). The proton

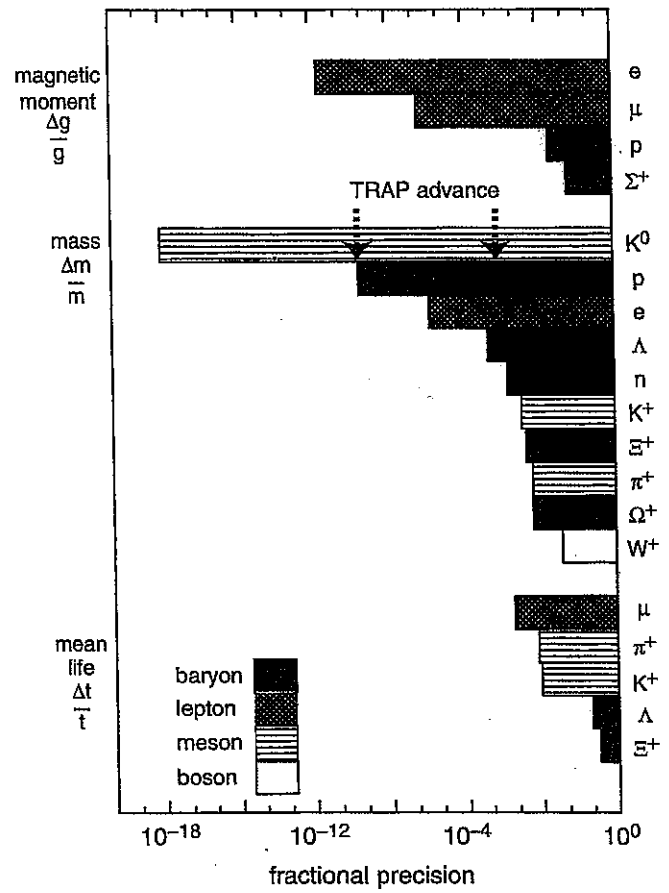

FIG. 2. Tests of CPT invariance.

(antiproton) is composed of three quarks (antiquarks) bound together. The K mesons, like all meson particles and antiparticles, are instead composed of a quark and an antiquark bound together. The third variety of particle is the lepton; the electron and the positron are examples of lepton particles and antiparticles. Leptons are not only not made of quarks, they seem to be perfect point particles since no experiment has yet detected any internal structure. It seems crucial to test CPT invariance in a sensitive way for at least one meson system, one baryon system and one lepton system.

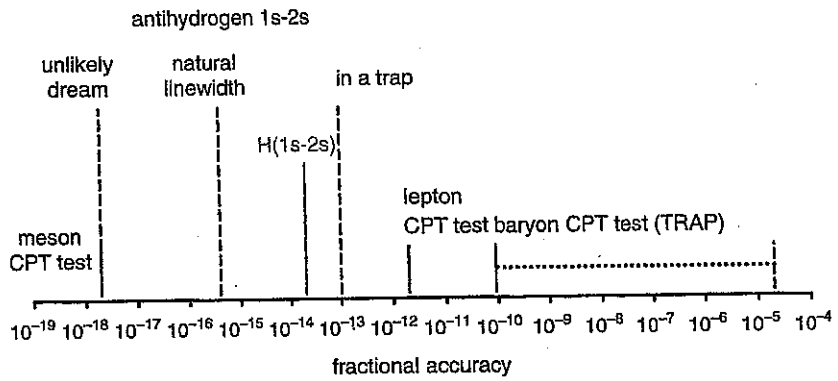

FIG. 3. Relevant accuracies for precise $\overline{\mathrm{H}}$ 1s–2s spectroscopy compared to the most stringent tests of CPT invariance carried out with the three types of particles: mesons, leptons, and baryons.

The motivation for comparing the antihydrogen 1s–2s transition frequencies is that the accuracy attained in measuring this interval in hydrogen (Cesar *et al.*, 1996; Niering *et al.*, 2000) is much higher than for any other CPT test involving leptons and baryons (Fig. 3). For example, the ratio of the Rydberg and the anti-Rydberg constants that could be deduced from such a measurement

$$\frac{R_\infty[\overline{\mathrm{H}}]}{R_\infty[\mathrm{H}]} = \frac{m[\mathrm{e}^+]}{m[\mathrm{e}^-]}\left(\frac{q[\mathrm{e}^+]}{q[\mathrm{e}^-]}\right)^2\left(\frac{q[\overline{\mathrm{p}}]}{q[p]}\right)^2\frac{1+m[\mathrm{e}^-]/M[p]}{1+m[\mathrm{e}^+]/M[\overline{\mathrm{p}}]} \tag{5}$$

depends upon all the ratios to the charges and masses (Hughes and Deutch, 1992) involved in antihydrogen and hydrogen. We hope and expect that such measurements will provide accurate CPT tests that are much more stringent than the most precise baryon and lepton CPT tests that are currently available.

The most accurate CPT test for a baryon system, by a large factor, is the 0.09 ppb (90×10^{-9}) comparison of q/m for the antiproton and proton (Gabrielse *et al.*, 1999b). Could it be that while the magnitude of q/m is the same for the antiproton and proton to an extremely high precision, that q and m for $\overline{\mathrm{p}}$ and p may differ in just such a way as to keep q/m the same? Our measurement of q/m, combined with a determination of q^2m for the $\overline{\mathrm{p}}$ (Hori *et al.*, 2003), shows that q and m separately have the the same mass and charge magnitude to an accuracy of 10 ppb – limited by the 100 times lower accuracy of the exotic atom spectroscopy that determines q^2m.

The most accurate CPT test for a lepton system is the comparison of the dimensionless magnetic moments or g values of the electron and positron, to a precision of 2 ppt (2×10^{-12}) (Van Dyck, Jr. *et al.*, 1987). At Harvard, we are just completing the first fully quantum measurement of the electron magnetic moment, using a one-electron quantum cyclotron (Peil and Gabrielse, 1999; D'Urso *et al.*, 2004). It looks like it may eventually be possible to get a positron-electron CPT test that is more than an order of magnitude more accurate.

How many atoms are really required for accurate $\overline{\mathrm{H}}$ spectroscopy? An experimental answer to this question is not yet available for either hydrogen or antihydrogen, but estimates suggest that small numbers may suffice (Zimmerman and Hänsch, 1993). My own suspicion is that the most accurate spectroscopy of both hydrogen and antihydrogen will ultimately be done with one atom at a time.

B. Extensions to the Standard Model that Violate Lorentz Invariance

Lorentz invariance violating extensions to the standard model have been considered and parameterized (Colladay and Kostelecký, 1997). Some of the possible terms cause CPT violations and some do not. The conclusion of a study of what could possibly be learnt from comparisons of hydrogen to antihydrogen (Bluhm *et al.*, 1999) is that high accuracy comparisons could provide substantial constraints on possible Lorentz-violating additions to the Standard Model.

C. Antihydrogen Gravity Tests

There have been no direct measurements of the gravitational acceleration of antimatter particles. This is not possible with charged particles because the gravitational force is so much smaller than the Coulomb force. With neutral antihydrogen there may be a chance, and it seems to me that a direct measurement would be interesting and very important. A neat review of gravitational theory and experiments summarizes the various indirect tests (Bell, 1987).

Our very accurate, 90 ppt (90 parts in 10^{12}) comparison of q/m for an antiproton and proton (Gabrielse *et al.*, 1999b) can be interpreted (Hughes and Holzscheiter, 1991) as a comparison of an antimatter clock (the cyclotron motion of antiproton) and a matter clock (the cyclotron motion of a proton). If the gravity acts differently on the the antimatter and matter clocks, then the gravitational red shift could make them run at different

rates. If the clocks run at the same rate to within 9×10^{-11}, as reported, then the accelerations due to gravity differ for antiprotons and protons by less than 1 ppm (1 part in 10^6).

A possibility that has generated much interest is that the familiar tensor gravity of our matter world, with its spin 2 graviton, might be accompanied by an attractive scalar contribution (spin 0 graviton) and repulsive vector contribution (spin 1 graviton), that happen to cancel for matter. For antimatter, however, the scalar and vector additions would both be attractive, so an $\overline{\mathrm{H}}$ atom would have a gravitational acceleration greater than the familiar value (Goldman *et al.*, 1986; Nieto and Goldman, 1991). It seems that equivalence principle experiments with ordinary matter set strict limits on the size of a possible vector contribution to gravity (Bell, 1987; Adelberger *et al.*, 1991), though the more detailed and recent version of this claim has generated some controversy (Adelberger and Heckel, 1991; Goldman *et al.*, 1991; Morpurgo, 1991).

Measuring gravitational properties of antihydrogen atoms seems to be difficult (Gabrielse, 1988; Walz and Hänsch, 2004) but is not excluded in principle. The relevant energy scales are summarized in Fig. 4. A significant challenge is that it is hard to cool $\overline{\mathrm{H}}$ atoms to the same low temperature that some other atoms can be laser-cooled. The Lyman alpha photons have more energy than the photons used to cool other atoms, and the $\overline{\mathrm{H}}$ atoms are less massive, so the laser cooling limit is higher.

One way that it may be possible to get lower temperature $\overline{\mathrm{H}}$ atoms would be to ionize extremely cold $\overline{\mathrm{H}}^+$ ions with a laser just above the ionization threshold (Walz and Hänsch, 2004). The challenge here is to produce the

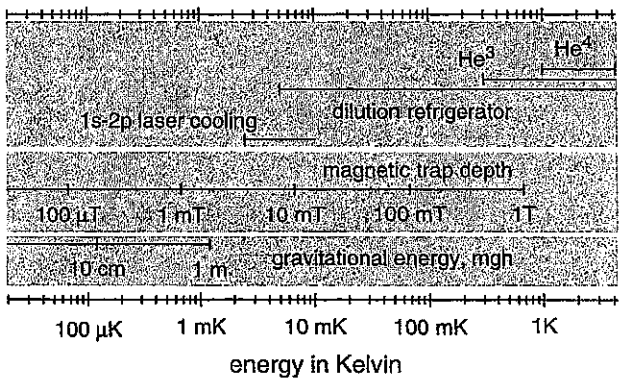

FIG. 4. Energies involved in the production, slowing and trapping of $\overline{\mathrm{H}}$ atoms along with the energy scale appropriate for gravitational experiments. Energies are specified in units of temperature. From (Gabrielse, 1988).

antimatter ions, not observed so far, and then to cool them to extremely cold temperatures, perhaps via collisions with laser cooled ions. I hope that we will find some $\overline{\mathrm{H}}^+$ if we look for them carefully, just as we found the trapped H^- ions that we used to compare q/m for the antiproton and proton (Gabrielse *et al.*, 1999b), but this may not work if hydrogen molecules were involved in H^- formation.

Of course, if the challenge of obtaining large numbers of μK and nK $\overline{\mathrm{H}}$ atoms can be met, then it could be that the now familiar free fall and atom interferometry experiments that can be carried out with laser cooled matter atoms, could be carried out with antihydrogen as well. Without a method to obtain such ultra-cold $\overline{\mathrm{H}}$ atoms, however, proposing to do such experiments seems like idle exercise.

III. Ingredients of Slow Antihydrogen

A. Cold Antiprotons for All Slow $\overline{\mathrm{H}}$ Experiments

The methods to accumulate 4.2 K $\overline{\mathrm{p}}$ are the basis of all efforts to produce and study cold antihydrogen. These techniques were developed by our TRAP Collaboration as summarized in the prequel (Gabrielse, 2001) to this review. Antiprotons with an energy of 5.3 MeV are ejected from a storage ring in a pulse that is typically 80 ns long. The crucial steps are

(1) Slowing the $\overline{\mathrm{p}}$ in a matter degrader (Gabrielse *et al.*, 1989a).
(2) Capturing the $\overline{\mathrm{p}}$ in a Penning trap by rapidly applying a trapping well while the $\overline{\mathrm{p}}$ are inside the trapping volume (Gabrielse *et al.*, 1986a).
(3) Electron-cooling of trapped $\overline{\mathrm{p}}$ (Gabrielse *et al.*, 1989b).
(4) Stacking $\overline{\mathrm{p}}$ from successive $\overline{\mathrm{p}}$ injection pulses (Gabrielse *et al.*, 1989b; Gabrielse, 2001; Gabrielse *et al.*, 2002c).

Some years later, some of these techniques were duplicated (Holzscheiter *et al.*, 1996) by the CERN PS-200 Collaboration that later developed into ATHENA.

Stacking $\overline{\mathrm{p}}$ from successive pulses of $\overline{\mathrm{p}}$ from the storage ring is now the only way to accumulate more than about 2×10^4 $\overline{\mathrm{p}}$ for current $\overline{\mathrm{H}}$ experiments. Accordingly we made a careful study of what is currently possible (Gabrielse *et al.*, 2002c), as summarized in Figs. 5 and 6.

The cold $\overline{\mathrm{p}}$ are readily stored in a cryogenic vacuum system. Our completely sealed and cold vacuum system produces the best vacuum used for $\overline{\mathrm{H}}$ experiments – so good that we needed to use $\overline{\mathrm{p}}$ as the vacuum gauge. We held $\overline{\mathrm{p}}$ for months awaiting collisions with background gas that would cause them to annihilate. No $\overline{\mathrm{p}}$ loss was detected, and the

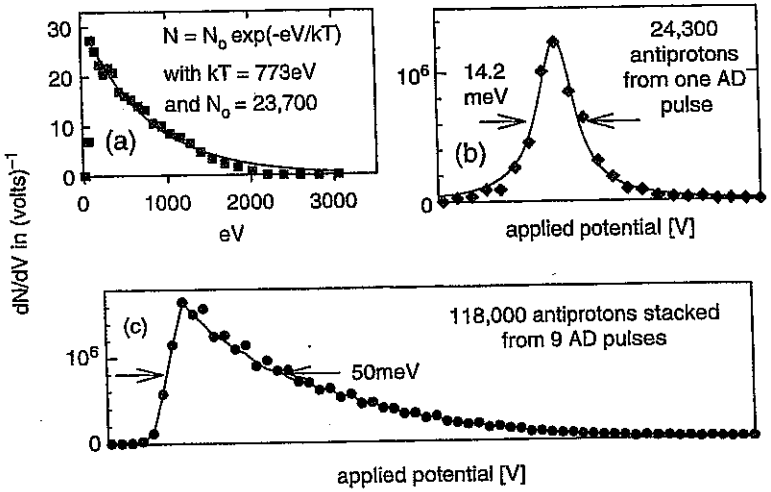

FIG. 5. Energy spectra for antiprotons trapped from a single pulse from the AD without (a) and with (b) electron cooling. Stacking (c) yields a much larger number of cold antiprotons. From (Gabrielse *et al.*, 2002c).

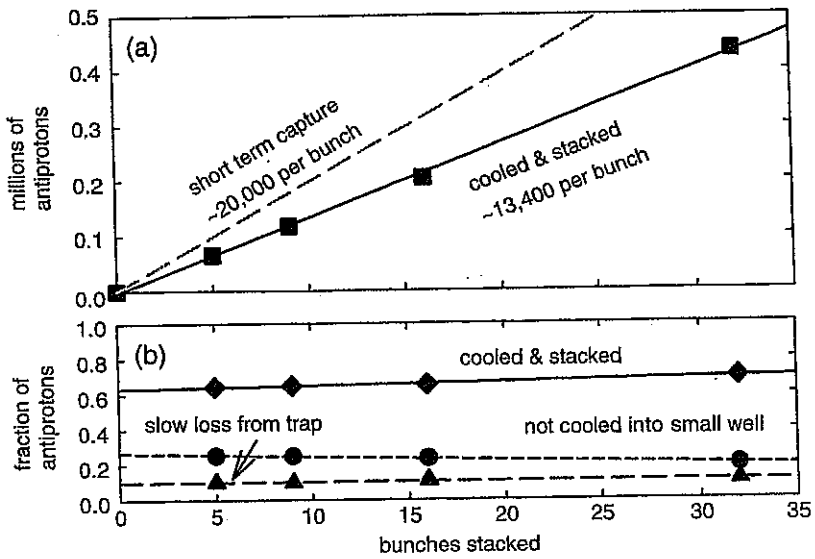

FIG. 6. Typical numbers of $\overline{p}$ that can be accumulated as a function of the number of $\overline{p}$ pulses that are delivered to a trap experiment – one pulse approximately every 80 s. From (Gabrielse *et al.*, 2002c).

uncertainty in the number of trapped $\overline{p}$ set a limit that the background pressure was less than 5×10^{-17} Torr (Gabrielse *et al.*, 1990). This high vacuum allows $\overline{H}$ experiments for which the annihilations of $\overline{p}$, e^+, and $\overline{H}$ are simply not a problem. For vacuum systems that are not completely cold, the pressure will of course be higher depending upon the area and condition of warm surfaces, upon how completely the trap volume is surrounded by cold surfaces, and by how much gas has been pumped onto these surfaces.

B. A New Storage Ring for Antihydrogen Experiments

The LEAR facility shut down after these $\overline{p}$ techniques were developed and demonstrated. The $\overline{p}$ techniques are now being used at a new storage ring – the Antiproton Decelerator (AD) – built at the CERN Laboratory in Geneva, Switzerland so that the envisioned $\overline{H}$ studies could be pursued. The AD replaces LEAR and two other storage rings that captured and accumulated $\overline{p}$ at high energies. With AD $\overline{p}$, and the TRAP techniques for accumulating cold $\overline{p}$, two international collaborations (soon to be three) are pursuing the mentioned objectives of precise spectroscopic comparisons of antihydrogen and hydrogen atoms. The AD sends about a hundred times less $\overline{p}$ to experiments in a single pulse of typically 3×10^7 (with 4.2×10^7 being the recent record high number). However, it sends more frequent pulses, about one every 80 s. The economy of the AD is possible because our $\overline{p}$ accumulation techniques make it possible to do the accumulation in a trap at low energies, rather than in a storage ring at high energies.

Not long before the LEAR ring was shut down, while we were busy developing the techniques that would make possible the production of slow $\overline{H}$ atoms, a small number of fast $\overline{H}$ atoms were produced and observed – first at CERN (Baur *et al.*, 1996) and then at Fermilab (Blanford *et al.*, 1998), as summarized in the Introduction. The incredible publicity that was afforded to these observations, in the scientific community and beyond, was a great help in promoting the construction of the CERN AD.

C. Better Efficiency with More Deceleration

Antiproton accumulation time could be greatly decreased if our $\overline{p}$ accumulation techniques could be applied after a decelerator first reduces the 5.3 MeV $\overline{p}$ energy of the $\overline{p}$ from the AD. Currently about 10^{-3} or less of the 5.3 MeV $\overline{p}$ from the AD storage ring are slowed in the degrader to

energies low enough that we can capture them in a trap (Gabrielse *et al.*, 2002c). If the $\bar{p}$ were first decelerated to lower energies, then less slowing in a degrader would be required. With a thinner degrader there would be less straggling energy width. A much higher fraction of the $\bar{p}$ could then be captured in a trapping well (of order 10 keV deep) that can be applied rapidly to capture the moving $\bar{p}$.

A radiofrequency quadrupole decelerator (RFQ) was proposed many years ago as a way to prepare $\bar{p}$ for traps (Coc *et al.*, 1991) but never realized. An RFQ is currently being inserted between the AD and a much thinner degrader by the ASACUSA collaboration (Yamazaki *et al.*, 2004). This is a very substantial and costly replacement for part of the thickness of the currently used degraders, and the low $\bar{p}$ acceptance of a RFQ places heavy demands on the AD and beam optics. However, the possibility to increase the number of $\bar{p}$ available for $\overline{H}$ experiments by one or two orders of magnitude is very attractive.

The hope is to eventually be able to exceed the 2×10^4 $\bar{p}$ at 4.2 K (Gabrielse *et al.*, 2002c) that are currently available for experiments from a single pulse of $\bar{p}$ from the AD. Antiprotons slowed in a decelerator will need to first be caught in a catching trap that is necessarily located right at the exit of the decelerator, and then transferred to an experiment trap. The number of $\bar{p}$ that can be cooled to 4.2 K within the experiment trap is the number that must be eventually compared to what is currently available for experiments from a single AD $\bar{p}$ pulse.

Alternately, a small but otherwise conventional storage ring could decelerate $\bar{p}$ after the AD. It would likely have a much larger acceptance than does a RFQ, but may be prohibitively expensive.

Both decelerator options could make possible a much more rapid accumulation of $\bar{p}$ into our trap for $\overline{H}$ experiments. The $\bar{p}$ that ATRAP now accumulates into its trap in an hour could likely be accumulated from a single injection of $\bar{p}$ from the AD. This would greatly speed up the rate at which experiments could be done, and in the future may make more $\overline{H}$ atoms available for spectroscopy. However, degraders are the currently available option, and these are extremely inexpensive and robust. It is also much easier to distribute $\bar{p}$ between experiments spaced far enough apart (so that their large magnetic fields do not greatly affect each other) at 5 MeV rather than at tens of keV.

D. Five Methods to Accumulate Cold Positrons

For slow $\overline{H}$ production, cold e^+ are needed as well as cold $\bar{p}$. Fortunately, e^+ from radioactive decay are readily available in any laboratory, unlike $\bar{p}$ whose production requires large accelerators. So far, ^{22}Na sources have been

used with five e^+ accumulation methods, four of which have produced cryogenic e^+ so far.

(1) At Harvard we used electronic damping to accumulate substantial numbers of 4.2 K e^+ (Haarsma *et al.*, 1995) for the first time, but the accumulation rate is slower than the methods currently used for $\overline{H}$ studies. It had been thought that electronic damping had been used previously to accumulate a few e^+ for precision measurements (Schwinberg *et al.*, 1981), but our work suggests that some other mechanism must be responsible.
(2) ATRAP developed and uses a method in which highly excited and highly magnetized positronium is produced and then ionized inside a trap that captures the e^+ (Estrada *et al.*, 2000; Gabrielse, 2001; Gabrielse *et al.*, 2001).
(3) ATHENA uses a method developed for plasma studies (Greaves *et al.*, 1994) in which fast e^+ collide with neutral gas atoms in a series of room temperature Penning traps with sequentially lower background gas pressures (Surko *et al.*, 1997; M. Amoretti, 2004).
(4) NIST demonstrated a method in which e^+ collide with laser-cooled Be^+ ions to be trapped and cooled (Wineland *et al.*, 1993; Jelenkovic *et al.*, 2003).
(5) A very thin and dense electron plasma has been used to slow e^+ for capture (Oshima *et al.*, 2003), but has not yet accumulated large numbers or low temperature e^+. It is hoped that this method could have the good vacuum of method 2 with the high accumulation rate of method 3.

Methods 2 and 3 are the most important in practice so far.

ATRAP's positronium method was the first to accumulate substantial number of cold (4.2 K) e^+. As currently used, up to 5×10^6 e^+ are available for experiments. These are accumulated during hours when $\bar{p}$ are not available for experiments, are hidden behind a rotatable electrode so as to be out of reach of $\bar{p}$ during $\bar{p}$ loading, are cleaned of ions by pulsing the e^+ from one electrode to another, and are reused from one $\overline{H}$ production experiment to another. Even for large numbers of e^+ the plasma is typically not so far from a spheroidal shape, as measured by an aperture method (Oxley *et al.*, 2004). In a trap with 1.2 cm working diameter we cannot currently handle many more e^+ in a robust way. The e^+ accumulation apparatus is very simple. Also, the e^+ and $\bar{p}$ accumulation take place entirely within coaxial trap electrodes that are completely surrounded by a 4.2 K vacuum enclosure. One result is that the e^+ cool naturally via synchrotron radiation to thermal equilibrium at 4.2 K. A second is that the vacuum inside the trap is better than the 5×10^{-17} Torr limit already discussed.

The gas slowing method adopted by ATHENA accumulates hot e^+ in a large and separate room temperature apparatus much more quickly, then transfers them several meters into the cold (15 K) $\overline{H}$ production region where they cool naturally via synchrotron radiation to 15 K. About 7.5×10^7 e^+ are stored in the larger ATHENA trap for $\overline{H}$ production experiments – about 15 times more e^+ than are typically used by ATRAP. The e^+ are distributed in a long thin plasma. Some radial compression comes from a rotating wall technique (Huang *et al.*, 1997; Anderegg *et al.*, 1998), and some from the entry of the e^+ into the strong field of a solenoid. The vacuum in the ATHENA apparatus is not as low as for ATRAP, owing to the coupling of warm and cold vacuum systems that is needed to admit e^+ into the cryogenic trap apparatus. However, the $\overline{p}$ lifetime is still much longer than needed for $\overline{H}$ production.

ATHENA can accumulate fresh e^+ to fill their larger diameter trap about every 5 min. ATRAP accumulates e^+ much more slowly, but reuses them over many hours. Especially when a mistake causes us to lose e^+, we at ATRAP are jealous of the rapid e^+ accumulation rate from buffer gas loading. Of course, what really matters is the number, density and plasma geometry of e^+ that are available for $\overline{p}$ experiments; the optimal value of these parameters for producing cold, ground state $\overline{H}$ is not yet known. It also remains to be seen if the better vacuum carefully preserved by the ATRAP approach will have advantages when precision measurements begin.

Cooling and trapping e^+ from a radioactive source by colliding them with laser cooled Be (Jelenkovic *et al.*, 2003) has yielded fewer e^+ ($\sim$2000) than was originally hoped for (Wineland *et al.*, 2003), though the number could likely be improved by using this method as a second step after one of the other e^+ accumulation mechanisms. An e^+ temperature limit < 5 K was established, substantially larger than the temperature of the ions. However, this temperature was realized in a room temperature apparatus. Also, very nice images clearly reveal centrifugal separation of the laser-cooled $^9Be^+$ ions and the e^+, with the e^+ compressed into a narrow column along a Penning trap's magnetic field axis, with density $\geq 4 \times 10^9$ cm^{-3}. The intriguing suggestion is made that, with better e^+ accumulation, it may be possible to use Mg^+ ions to cool up to 10^9 e^+ to similar low temperatures within a room temperature apparatus.

E. Plasma Diagnostics

A quantitative understanding of $\overline{H}$ production requires a good understanding of the density and geometry of the $\overline{p}$ and e^+ plasmas from which

$\overline{H}$ forms. The number of trapped particles is relatively easy to measure. Trapped $\overline{p}$ released from the trap produce annihilation signals in surrounding scintillators that can be counted. Trapped e^+ released from the trap produce a measurable current when they strike an electrode.

In a perfect electrostatic quadrupole potential, trapped particles in a Penning trap will fill a spheroid (an ellipsoid with cylindrical symmetry about the magnetic field direction) which has a uniform density essentially out to its boundary (Dubin and O'Neil, 1999). If the number of particles is measured, then one more parameter is needed to determine the density and spatial distribution of the charges in the spheroid.

At ATRAP we have measured the additional parameter for both e^+ and $\overline{p}$ plasmas by measuring the number of charges that make it through an aperture whose radius is smaller than the radius of the plasma (Oxley *et al.*, 2004). This is the only method to measure the distribution of $\overline{p}$ in a trap so far.

Real traps do not produce perfect electrostatic quadrupole potentials especially near the walls of traps made from cylindrical rings, even when the geometry of such traps is carefully chosen (Gabrielse *et al.*, 1989c). It is thus by no means clear that trapped plasmas will form ideal spheroidal plasmas. A nice feature of the aperture method is that it does not require assumption that the charges form a spheroid distribution. In fact, the $\overline{p}$ distribution that we measured was not well-approximated by a spheroid.

Both ATRAP (Estrada *et al.*, 2000) and ATHENA (Amoretti *et al.*, 2003) detect the radiofrequency currents induced by the oscillation of the e^+ center-of-mass along the magnetic field direction, as a nondestructive alternative to measuring the number of e^+ by ejecting them from the trap. (The familiar center-of-mass oscillation of trapped charges that for decades has been used to nondestructively measure the number of trapped particles is sometimes now referred to rather obliquely as the lowest hydrodynamic mode.) Using the induced radiofrequency current is fine as long as this calibration is checked often against the actual number deduced directly using the ejecting the e^+. Care must be taken because we have observed that for large numbers of e^+ the induced radiofrequency current can depend significantly upon the distribution of charges in the trap.

Another way to measure the additional parameter needed to characterize the density and spatial distribution of a trapped plasma is to measure the oscillation frequencies for internal hydrodynamic oscillation modes of the trapped plasma. These frequencies have been calculated for ideal spheroidal plasmas (Dubin, 1991), and were studied in wonderful detail for plasmas of trapped ions (Bollinger *et al.*, 1993). Later, this method was used to analyze trapped electrons (Weimer *et al.*, 1994) and then trapped e^+ (Tinkle *et al.*, 1996).

Shifts in the lowest frequency internal oscillation mode have been used to measure increases in the e^+ plasma temperature (M. Amoretti, 2003; Amoretti *et al.*, 2003), from an initial unmeasured value that is assumed to be the temperature of the trap electrodes. A spheroidal e^+ is assumed.

Annihilation "imaging" has been used to learn about the loss of stored $\overline{p}$ (Fujiwara *et al.*, 2004), though the spatial resolution with which the $\overline{p}$ annihilation vertex was measured is unfortunately not much smaller than the trap radius. However, it sufficed to show that all $\overline{p}$ ejected from the trap annihilated at discrete patches on the surface of the trap electrodes. The cylindrical symmetry of the Penning trap used about the magnetic field direction is thus broken by something. Whether this is a feature of the imperfections in this particular trap, or whether such imperfections are present in all traps, is not clear.

IV. Production Method I: During e^+ Cooling of $\overline{p}$ in a Nested Penning Trap

A. Nested Penning Trap and Positron Cooling of Antiprotons

The production of cold $\overline{H}$ requires the interaction of $\overline{p}$ and e^+. Their opposite sign of charge makes it impossible for them to share the same potential well in a Penning trap, since one of the two species will see it as a potential hill. Many years ago the nested Penning trap was proposed as a solution (Gabrielse *et al.*, 1988). Figure 1 in the Introduction and Overview shows $\overline{p}$ in a large outer well, with e^+ in the inverted central well. (Of course, it would be possible to reverse the particle locations by inverting the potential, as may be desirable to get colder $\overline{H}$.) Essentially all of the large number of slow $\overline{H}$ produced by ATRAP and ATHENA so far were produced in a nested Penning trap, during the e^+ cooling of $\overline{p}$, since ATRAP has only recently demonstrated the second production method (Sect. VII).

Electrons and protons were used to first demonstrate cooling of oppositely charged species in a nested Penning trap (Hall and Gabrielse, 1996). Figure 8 shows the spectrum of protons with and without cooling electrons in the center of the nested Penning trap (Fig. 7). Without cooling electrons in the central well, hotter protons retain the higher energy distributions illustrated to the right in the figure. With cooling electrons in the well the proton energy spectrum cools dramatically as shown to the left in the figure.

The next big step was to get $\overline{p}$ and e^+ into such a trap structure and demonstrate their interaction (Gabrielse *et al.*, 1999a). Figure 9 represents

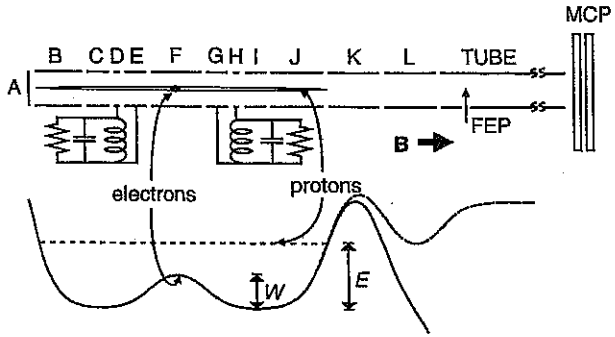

FIG. 7. Scale outline of the inner surface of the electrodes (a), and the potential wells (b), for the nested Penning trap. (Taken from (Hall and Gabrielse, 1996).)

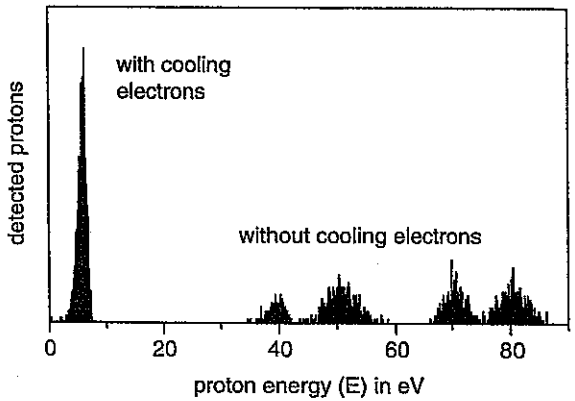

FIG. 8. Energy spectrum of the hot protons (right) and the cooled protons (left), obtained by ramping the potential on electrode K downward and counting the protons that spill out to the channel plate detector. (Taken from (Hall and Gabrielse, 1996).)

the nested Penning trap used, the $\overline{p}$ and e^+ locations, and the electrical signals that tell us the number of $\overline{p}$ and e^+ in the trap. Figure 10 shows that e^+ are heated when $\overline{p}$ pass through them. This demonstration was made during the last week of LEAR's operation.

B. Demonstration and Study of Positron Cooling of Antiprotons

The first e^+ cooling of $\overline{p}$ was demonstrated by ATRAP at the AD (Gabrielse *et al.*, 2001). Figure 12(a) shows the measured energy spectrum when no e^+ are in the center of a nested Penning trap. Figure 11(b) shows a spectrum of

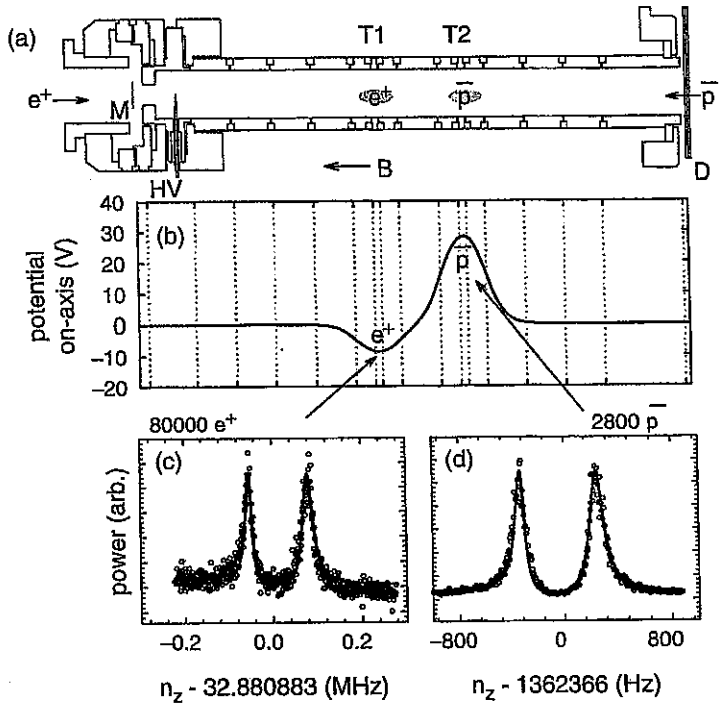

FIG. 9. (a) Electrode cross sections and the initial position of the simultaneously trapped e^+ and e^-. (b) Trap potential on the symmetry axis. Fits (solid curves) to the electrical signals from simultaneously trapped e^+ (c) and $\bar{p}$ (d) establish the number of trapped particles. From (Gabrielse *et al.*, 1999a).

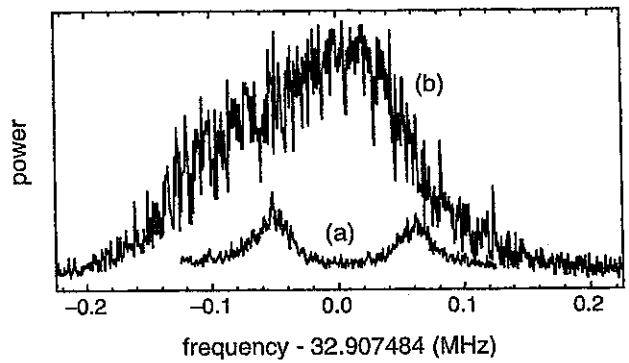

FIG. 10. The signal from cold trapped e^+ (below) changes dramatically (above) when heated $\bar{p}$ pass through cold e^+ in a nested Penning trap, showing the interaction of $\bar{p}$ and e^+. From (Gabrielse *et al.*, 1999a).

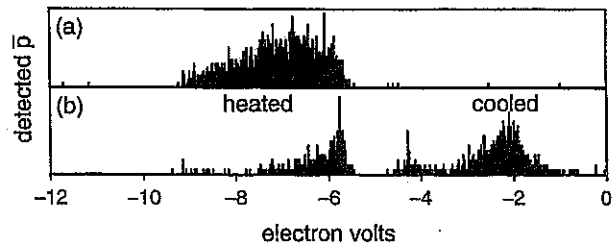

FIG. 11. First e^+ cooling of $\bar{p}$ is demonstrated by the axial well depth at which $\bar{p}$ escape the trap without (a) and with (b) e^+ cooling. From (Gabrielse *et al.*, 2001).

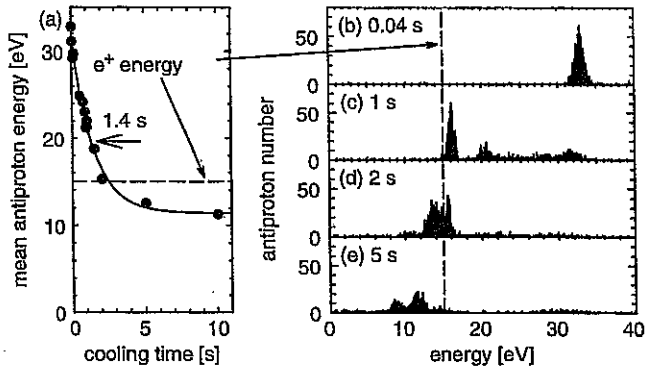

FIG. 12. More detailed e^+ cooling spectrum. From (Gabrielse *et al.*, 2002a).

$\bar{p}$ that are cooled (i.e., shifted right in the figure) by e^+ in the center of the nested well. The uncooled $\bar{p}$ (left in Fig. 11(b)) do not pass through the e^+ plasma. The little central peak in this example are $\bar{p}$ that are going through the e^+, with the right energy to form $\overline{H}$. Undoubtedly $\overline{H}$ atoms were formed here.

The $\bar{p}$ peak to the right in Fig. 11(b) reveals $\bar{p}$ that are cooled below the energy that takes them through the e^+, with a cooling time that is about ten times longer than the initial $\bar{p}$ cooling time. The process seems to be a lossless evaporative cooling. The $\bar{p}$ in the side wells of the nested Penning trap that acquire enough energy in $\bar{p}$–$\bar{p}$ collisions will again pass through the e^+ and be cooled, rather than evaporating completely out of the trap. These $\bar{p}$ can be brought back into contact with the e^+ to make more $\overline{H}$ (Sect. IV.C).

Because of the importance of e^+ cooling of $\bar{p}$ in the nested trap for $\overline{H}$ production we carried out a careful and detailed study of this process in 2002. Figures 12(b–e) shows examples of the $\bar{p}$ energy spectra after various

cooling times. Figure 12 shows the average $\bar{p}$ energy as a function of e^+ cooling time, before the $\bar{p}$ cool into maximum contact with the e^+. The subsequent lossless evaporative cooling of the $\bar{p}$ takes places on a much longer time scale. Details of ATRAP's progress in quantitatively understanding the e^+ cooling of $\bar{p}$ in a nested Penning trap was reported in a thesis (Bowden, 2003). Figure 13 shows $\bar{p}$ cooling as a function of their time in contact with the e^+, and the calculated cooling using a theory developed to describe cooling in a nested Penning trap (Chang and Ordonez,

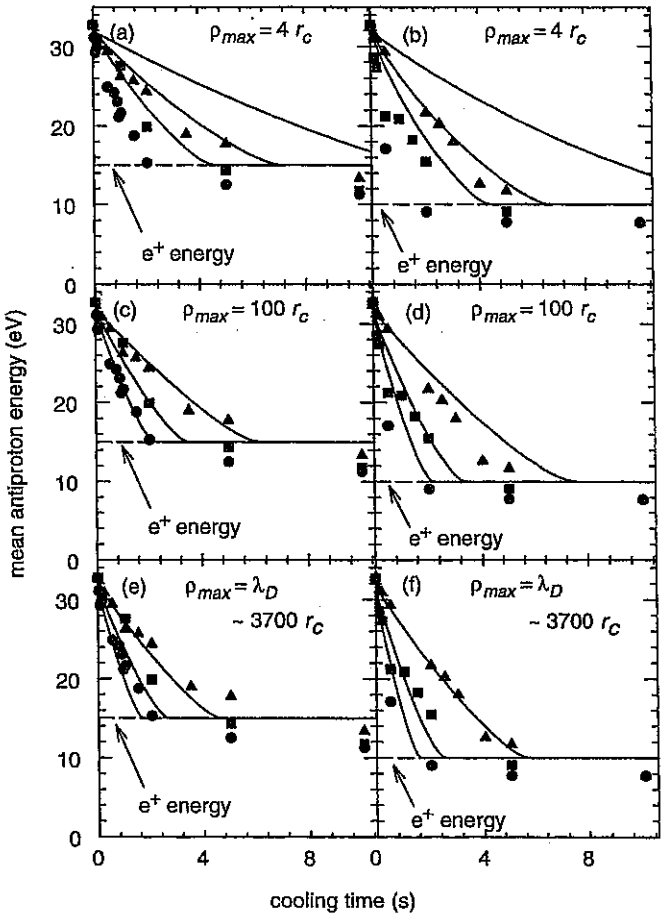

FIG. 13. Rate of antiproton axial energy loss depends on number of positrons placed in either a 15 V (a) or 10 V (b) well. Solid curves are exponential fits to the data. From (Bowden, 2003).

2000). The vertical sequences show quantitative agreement between theory and experiment, but only when we greatly increased a crucial cut off length from a value near the thermal cyclotron radius that was suggested in the theoretical treatment, to nearer to the Debye length, which seems to be a better choice given that axial energy is being transferred. A related theory paper has just been published (Chang and Ordonez, 2004). There are also several papers which focus on the interaction of a $\bar{p}$ plasma with a e^+ plasma (Ordonez, 1997; Ordonez *et al.*, 2002).

Very recently, ATHENA reported observations of the e^+ cooling process (Amoretti *et al.*, 2004) that are similar to the examples shown in Figs. 11 and 12, except that the $\bar{p}$ cool faster with more e^+, as expected.

C. A Variation: Driven e^+ Cooling of $\bar{p}$

ATRAP and ATHENA's first $\overline{H}$ observations (M. Amoretti *et al.*, 2002; Gabrielse *et al.*, 2002a), and all of ATHENA's subsequent $\overline{H}$ experiments, produced $\overline{H}$ using the simplest, one-time realization of e^+ cooling of $\bar{p}$. The $\bar{p}$ were injected into a nested Penning trap that contained e^+, and were cooled by the e^+ until all cooling and all $\overline{H}$ production stopped.

Almost immediately, ATRAP moved to driven $\overline{H}$ production (Gabrielse *et al.*, 2002b), in which $\bar{p}$ are driven through repeated cycles of e^+ cooling. This variation is an improvement for two reasons.

(1) More $\overline{H}$ are produced for a given number of $\bar{p}$.
(2) Antiprotons can be given no more energy than is required for them to barely move through the e^+ plasma, to form $\overline{H}$ atoms.

The careful optimization needed to realize the second advantage is now being attempted.

To drive the production of slow $\overline{H}$ (Gabrielse *et al.*, 2002b), $\bar{p}$ in the right potential well are heated with a resonant radiofrequency drive until they pass through the e^+ in the inverted central well. Collisions of $\bar{p}$ and e^+ (which cool to 4.2 K via synchrotron radiation) cool the $\bar{p}$ until they settle into the left well of the nested trap. The resonant heating drive is then switched to heat the $\bar{p}$ out of the left well, so the e^+ in the center can cool them back into the right well. There is detectable $\bar{p}$ loss during the driving sequence (Fig. 14). Slow $\overline{H}$ atoms are produced during such repeated cycles of e^+ cooling of $\bar{p}$.

The number of $\overline{H}$ produced during each drive cycle is linear in the number of $\bar{p}$ in the trap (Fig. 15(a)). A small $\bar{p}$ remnant is presumably unable to form $\overline{H}$ because of poor spatial overlap with the e^+. The number of $\bar{p}$ in the trap, and hence the number of $\overline{H}$ detected, decreases

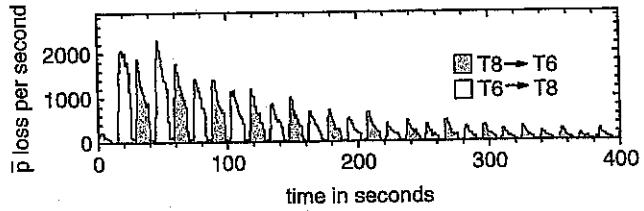

FIG. 14. Antiprotons lost while being driven from one side of the nested Penning trap to the other. From (Gabrielse *et al.*, 2002b).

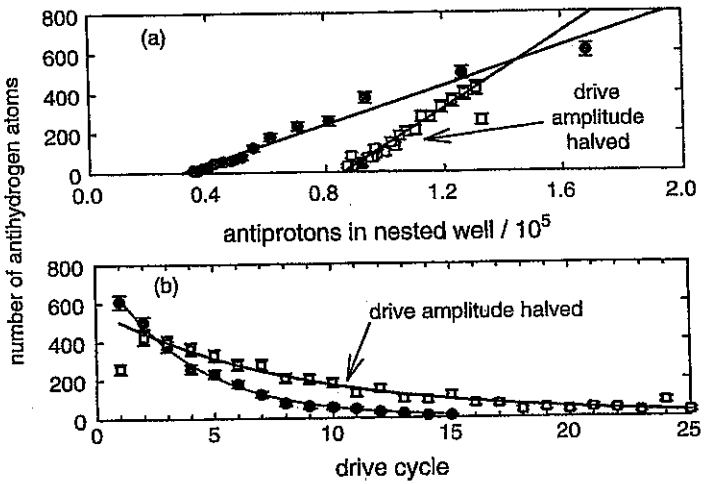

FIG. 15. The number of $\overline{H}$ atoms detected is linear in the number of $\bar{p}$ in the trap (a), even as it decreases as a function of drive cycle because of $\bar{p}$ losses (b).

exponentially with the number of drive cycles (Fig. 15(b)). The drive apparently heats the $\bar{p}$ so that some diffuse radially out of the trap, but this is not well-understood.

The strong drive we typically used (Gabrielse *et al.*, 2002b) is represented by filled squares in Fig. 15. Even stronger drives, likely to reduce the small remnant, were avoided for fear of producing $\overline{H}$ with higher velocities. A weaker drive, half the strength of the first, produces $\overline{H}$ less rapidly to start with, produces about twice as much detectable $\overline{H}$ integrated over all drive cycles, and leaves a larger $\bar{p}$ remnant (open squares in Fig. 15). Further reductions in drive strength decrease $\overline{H}$ production roughly in proportion to the drive amplitude, without changing the number of remnant $\bar{p}$ that remain out of contact. Slowly

increasing the drive amplitude during each cycle could minimize the speed of the $\overline{H}$ produced, and more sophisticated variations of drive amplitude and frequency are being considered.

D. Antiproton Losses from a Nested Penning Trap

One issue that prompted ATRAP to develop its background-free detection method (Sect. IV.E) was the observation of radial $\bar{p}$ losses from a nested Penning trap. These losses take place during the e^+ cooling of $\bar{p}$. In fact, they take place when the $\bar{p}$ have cooled to the energies which just take them through the e^+ plasma in the center of the nested Penning trap. At first it was tempting to identify them as $\overline{H}$ atoms that leave the trap upon forming, until we demonstrated that such $\bar{p}$ losses can take place with no e^+ in the nested Penning trap.

This $\bar{p}$ loss unfortunately only takes place when the $\bar{p}$ have the energy close to that which takes them just over the potential hill from the empty e^+ trap. Typically if $\bar{p}$ are loaded into a nested Penning trap that contains no e^+, then the $\bar{p}$ will not cool down to the energies which take them just over the potential hill that the empty e^+ well presents to them, with the result that no $\bar{p}$ losses will be observed. This is also true if the e^+ cooling would be turned off by heating the e^+ in a nested Penning trap to high temperature. At ATRAP we observed these losses in two ways. First, we waited for a much longer time that was required for e^+ cooling. Collisions between the $\bar{p}$ spread out their energies, with some of the $\bar{p}$ distribution being at energies where the $\bar{p}$ loss could take place. Second, we heated $\bar{p}$ in the side wells of the nested Penning trap to give them energies that took them over the central well for e^+ (Fig. 14).

ATHENA does not report such losses. Is this because their e^+ are stored much farther from trap walls? Or, is it because very highly excited $\overline{H}$ atoms are formed from rapidly moving $\bar{p}$ before the e^+ cool them to the lower energies at which some would be lost from the trap? Or, is there another explanation?

E. Two Techniques to Count $\overline{H}$ Atoms

As reported first in 2002, two different techniques are used to count the $\overline{H}$ atoms that are produced during e^+ cooling of $\bar{p}$ in a nested Penning trap. ATRAP uses field ionization detection (Gabrielse *et al.*, 2002a,b) and ATHENA uses correlated loss detection (Amoretti *et al.*, 2002). After a brief summary of each detection technique, the two are compared.

E.1. ATHENA's $\overline{H}$ annihilation detection

ATHENA adopted the nested Penning trap and the e^+ cooling of $\bar{p}$ method to produce $\overline{H}$, but counted the atoms very differently than did ATRAP – detecting the correlated loss of $\bar{p}$ and e^+ from the nested trap (Amoretti *et al.*, 2002). Upon forming, a neutral $\overline{H}$ is no longer confined and thus starts its drift to the electrodes of the nested Penning trap. When the $\overline{H}$ strikes a trap electrode, its $\bar{p}$ and its e^+ will annihilate at essentially the same time. A $\bar{p}$ and a e^+ annihilation taking place at the same place thus seems to be a unique signature of $\overline{H}$ annihilation.

Real detectors do not have perfect space or time resolution, however. ATHENA's $\overline{H}$ annihilation detection (Amoretti, 2004) thus counted any $\bar{p}$ and e^+ annihilation that took place within 5 μs and ±8 mm of each other as an $\overline{H}$ atom. The resolution is very modest compared to a state-of-the-art particle detector; it is limited by the very small space available for a detector that needs be near a cold trap. Silicon strips are used to detect the pions from $\bar{p}$ annihilations, and CsI crystals are used to detect the back-to-back photons from e^+ annihilation.

Unfortunately, false $\overline{H}$ events arise when a $\bar{p}$ annihilates, even when the $\bar{p}$ is not bound in an $\overline{H}$. Neutral pions are one product of $\bar{p}$ annihilation, and neutral pions decay into electron-positron pairs. In this way a $\bar{p}$ and a e^+ annihilation will occur within the time resolution of any detector. If the $\bar{p}$ and a e^+ (from $\bar{p}$ annihilation) both annihilate within the spatial resolution of the detector as well, then the false event cannot be distinguished form a real $\overline{H}$ annihilation. Is a spatial resolution of ±8 mm sufficient to eliminate false $\overline{H}$ events from $\overline{H}$ that leak out of the trap at the same energies that $\overline{H}$ atoms are expected to form?

Apparently the answer is yes. Only weeks after first duplicating e^+ cooling of $\bar{p}$ in a nested Penning trap, ATHENA counted 131 "golden" $\overline{H}$ events on top of a large background (Amoretti *et al.*, 2002). With some time to study the performance of the detector, they have very recently argued that many of the background events are also real $\overline{H}$ counts (Amoretti *et al.*, 2004).

E.2. ATRAP's dield ionization detection

ATRAP's field ionization detection is very different. Any $\overline{H}$ atom formed near the center of a nested Penning trap is free to move in the initial direction of its $\bar{p}$, unconfined by the nested Penning trap. $\overline{H}$ atoms passing through the ionization well (sometimes called a detection well) in a state that can be ionized by the electric field within, will leave their $\bar{p}$ trapped in this well.

The ionization well (within electrode EET in Fig. 16(a)) is carefully constructed so that its electric field ensures that no $\bar{p}$ from the nested

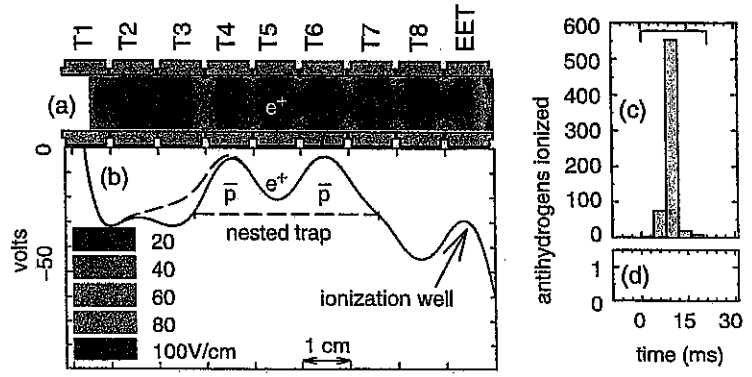

FIG. 16. (a) Electrodes for the nested Penning trap have an inner diameter of 1.2 cm. Inside is a representation of the magnitude of the electric field that strips $\overline{H}$ atoms. (b) The potential on axis for positron-cooling of antiprotons (solid) during which $\overline{H}$ formation takes place, with the (dashed) modification used to launch $\bar{p}$ into the well. (c) Antiprotons from $\overline{H}$ ionization are released from the ionization well during a 20 ms time window, (d) No background $\bar{p}$ are counted when no e^+ are in the nested Penning trap. From (Gabrielse *et al.*, 2002a).

Penning trap can get into it (e.g., a $\bar{p}$ liberated from the nested well by ambipolar diffusion) except if it travels about 4 cm bound within an $\overline{H}$ atom. Any $\bar{p}$ heated out of the nested Penning trap escapes over the lower potential barrier in the other direction. Even if a $\bar{p}$ did acquire enough energy to go over the ionization well in one pass it would not be trapped because there is no mechanism to lower its energy while over this well. In addition, e^+ cooling lowers the energy of the $\bar{p}$ in the nested well, taking them further from the energy required to even pass over the ionization well.

Only signals from $\overline{H}$ are detected with this field-ionization method (Gabrielse *et al.*, 2002a) – there is no background at all! Figure 16(c) shows ionized $\overline{H}$ captured in the ionization well during the course of the one initial experiment. In trials without e^+, no $\bar{p}$ was detected in the ionization well (Fig. 16(d)). Antiprotons from $\overline{H}$ ionization are stored in the ionization well until after e^+ cooling is completed in the nested well, and all other $\bar{p}$ and e^+ are released in the direction away from the ionization well. We then eject the trapped $\bar{p}$ by ramping down the potential of the ionization well. The ejected $\bar{p}$ annihilate upon striking electrodes, generating pions and other charged particles that produce light pulses in the surrounding scintillators.

E.3. Comparing the detection techniques

There are advantages and disadvantages to both the detection techniques. ATHENA detects the correlated loss of $\bar{p}$ and e^+ from the nested Penning

trap. This technique has the advantage that $\overline{H}$ atoms with any internal state and any velocity should be detected, reduced by the efficiency of the detection process. The disadvantage is that it is thus difficult to learn about either the internal state of the $\overline{H}$, or about the velocity of the $\overline{H}$. The count rate for the golden events is quite low, and it seems likely that $\bar{p}$ detection will often be used in the future without e^+ detection.

ATRAP's field ionization detection has the advantage of being background free, making it possible to detect very small signals if needed. Field ionization detection also makes it possible to go beyond counting $\overline{H}$ atoms (Sect. V), and the $\overline{H}$ internal state and the $\overline{H}$ center-of-mass velocity have already been probed. The disadvantage is that only excited atoms that can be field ionized are detected. We hope to use lasers to excite more deeply bound states up to excited states that can be detected by field ionization, but this remains to be demonstrated.

As the time of $\overline{H}$ trapping (Sect. IX.A) approaches, the substantial metal supports for superconducting coils or permanent magnets needed near to the trap may make it impossible to spatially resolve the location of $\bar{p}$ and e^+ annihilations. The scattering of charged pions from $\bar{p}$ annihilation in this material, and the increased attenuation of the photons from e^+ annihilation, will make the marginal spatial resolution achieved so far to be much worse. ATRAP thus committed to developing alternate $\overline{H}$ detection techniques from the outset.

V. Beyond Counting $\overline{H}$ Atoms

A. Probing Internal $\overline{H}$ Orbits

The basic idea of the field ionization method used by ATRAP to probe the internal structure of $\overline{H}$ atoms is represented in Fig. 17. A small fraction of

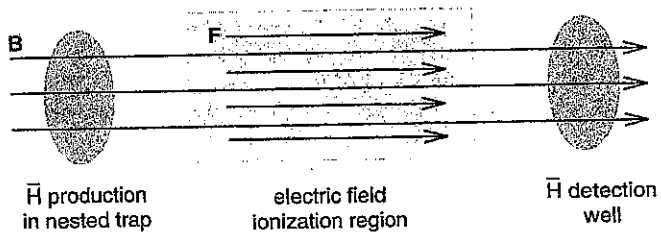

FIG. 17. $\overline{H}$ atoms created in within a nested Penning trap must pass through an electric field region to reach and be counted in the detection well. Any $\overline{H}$ that is field ionized in this electric field region will not be detected in the detection well.

the $\overline{H}$ atoms produced in the nested Penning trap travel along the magnetic field direction to the right in Fig. 17 – passing first through an electric field F_z parallel to the magnetic field, and then into the detection trap volume. They are counted if they survive F_z without ionizing and are instead ionized by the stronger electric field in the detection trap. $\overline{H}$ ionized in the detection well leave their $\bar{p}$ in this well until we release them and count the $\bar{p}$ annihilations in surrounding scintillators – thereby detecting $\overline{H}$ with a detection efficiency of about 0.5 and no background. In Sect. V.C we discuss the example of a field ionization spectrum in Fig. 21.

A recent theory paper (Vrinceanu *et al.*, 2004) discusses field ionization in a strong magnetic field, and suggests the use of radial size as the best way to specify the state of a highly excited, highly magnetized $\overline{H}$ atom. The largest atoms detected are guiding center atoms (GCA) (Glinsky and O'Neil, 1991), and a circular GCA is represented in Fig. 18(a). Figure 18(b) shows how such atoms polarize and then field ionize as F_z increases. Figure 18(c) illustrates how the ionization potential depends upon the axial energy as well as the drift radius of the atom.

Figure 19 shows that for various analytic and numerical models of GCA atoms, and also for atoms that are too tightly bound to be described in this way, that the electric field F_z at which the atoms ionize is a reliable indication of their radial size ρ. Atoms that survive an electric field F_z must have a radial size

$$\rho \leq \frac{a}{\sqrt{F}}\sqrt{\frac{e}{4\pi\varepsilon_0}}, \tag{6}$$

with $a=0.5$ a good rule of thumb (Vrinceanu *et al.*, 2004) for the experimental circumstances. This is only a rule of thumb in that the axial binding decreases as the axial energy increases.

A more detailed theoretical consideration of GCA atoms in electric fields is just being reported (Kuzmin and O'Neil, 2004b). It agrees with our $\overline{H}$ polarization and field ionization analysis for parallel electric and magnetic fields described above (Vrinceanu *et al.*, 2004), and extends these results in two ways. First, an explicit form for the dependence of the ionization field upon axial energy is presented, a dependence illustrated in our Fig. 18(c). Second, the $\overline{H}$ polarization and the modifications of the $\overline{H}$ center-of-mass trajectory due to radial electric fields are both explored.

B. Measured Field Ionization Spectrum

The number of $\overline{H}$ atoms formed increases in proportion to the number of e^+ that we use to form them (Fig. 20). Under ATRAP experimental conditions,

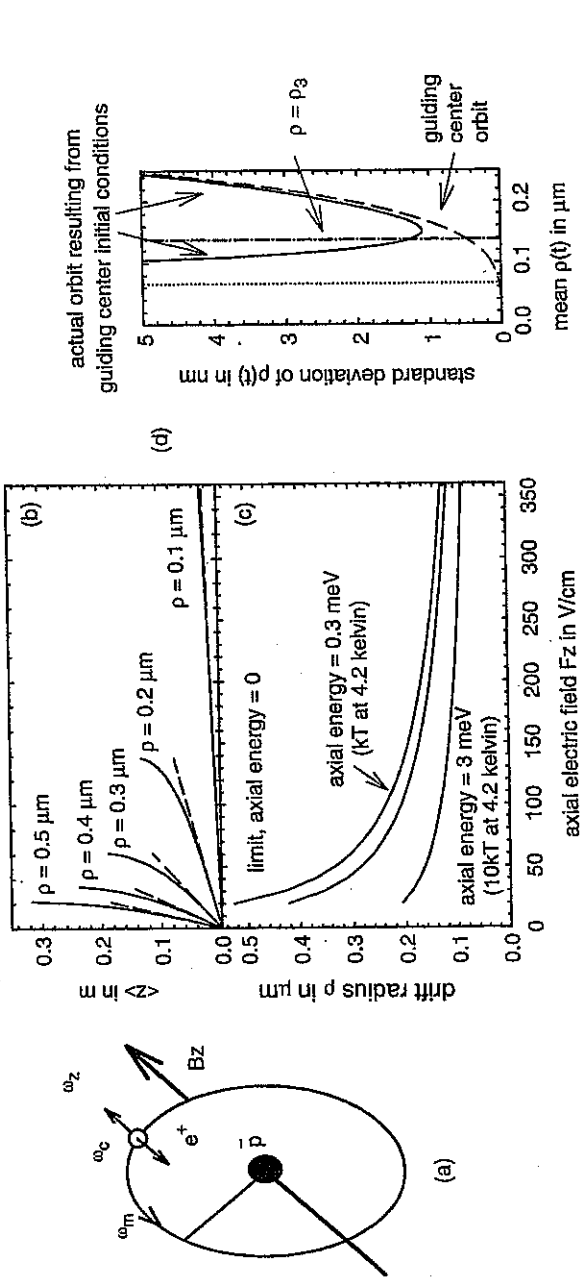

FIG. 18. A circular guiding center $\overline{H}$ atom (a) is polarized (b) and ionized (c) by an electric field F is applied along B. Without an ionizing field, the GCA approximation breaks down at $\rho \approx \rho_3$ (d). Parts (a)–(c) are from (Vrinceanu *et al.*, 2004). Part (d) is from (Gabrielse *et al.*, 2004a).

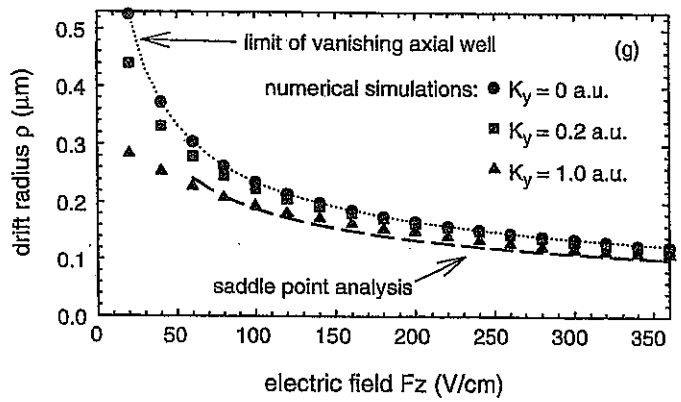

FIG. 19. The field at which an excited $\overline{H}$ ionizes establishes an upper limit upon its radial size. From (Vrinceanu *et al.*, 2004).

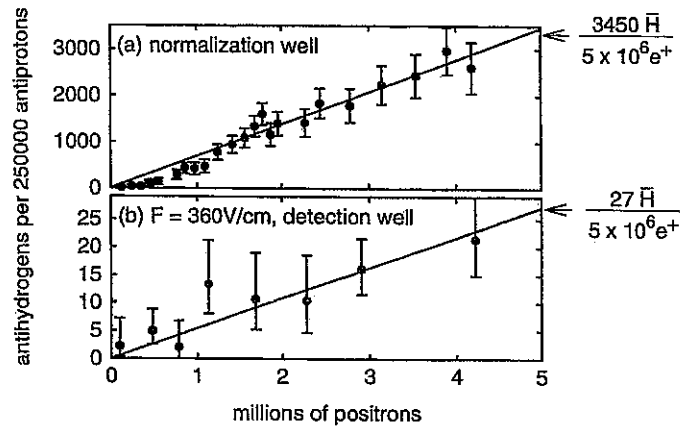

FIG. 20. $\overline{H}$ Produced from 2.5×10^5 $\bar{p}$ and detected in the normalization (a) and detection wells (b), the latter having survived a 360 V/cm field without ionizing. From (Gabrielse *et al.*, 2004a).

the number of e^+ is roughly proportional to the thickness of the e^+ plasma along the magnetic field direction. From such measurements we construct the field ionization spectrum in Fig. 21. This spectrum shows that the number of $\overline{H}$ atoms that survive F_z decreases approximately as F_z^{-2} for atoms appropriately described as GCA (shaded region), indicating that the number of $\overline{H}$ that ionize at F_z goes as F_z^{-3}.

A simple argument, perhaps too simple, gives such a dependence. We might suppose that the initial three body capture varies as ρ^4 since two e^+

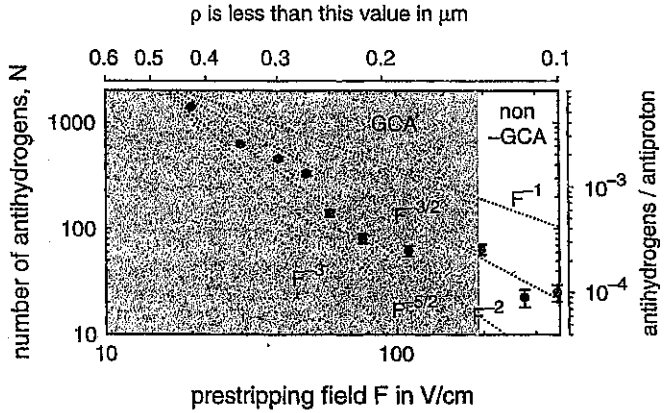

FIG. 21. Number N of $\overline{\mathrm{H}}$ that survive an ionization field $F = F_z$, for 2.5×10^5 $\bar{\mathrm{p}}$ and $5 \times 10^6 \mathrm{e}^+$, taken from measurements such as shown in Fig. 20. From (Gabrielse *et al.*, 2004a).

are involved in the formation, and that a subsequent deexcitation collision (between the bound e^+ and another e^+ in the plasma) has a rate that goes as ρ^2. This would suggest that the number of $\overline{\mathrm{H}}$ that ionize at F_z goes as $\rho^6 \sim F_z^{-3}$, as is observed. This argument, however, does not give a careful account of the velocity dependence of these rates, nor upon details of the formation and deexcitation process.

For the largest F_z, however, just where the GCA should be breaking down (as we shall see in the following section), the number of $\overline{\mathrm{H}}$ atoms seems like it may be larger than the power law trend. There is not yet any theoretical model which predicts either the power law trend nor any departure from it for more tightly bound atoms.

It has been suggested (Driscoll, 2004) that our first field ionization spectrum (Gabrielse *et al.*, 2002b) is well-described by a simulation of three body formation (Glinsky and O'Neil, 1991). This would be wonderful, but unfortunately does not seem to be so (Gabrielse *et al.*, 2004) (and would be even less so for the much bigger range of F_z in Fig. 21). The simulation illustrates basic features of three body formation in a strong magnetic field very well, but was not intended to generate spectra that could be compared experimentally. Simulation results were thus simply not reported for a wide enough range of $\overline{\mathrm{H}}$ binding energies. A more extensive simulation could possibly solve this problem and would also provide the opportunity to add in the important coupling between internal and center-of-mass motions (Vrinceanu *et al.*, 2004; Kuzmin and O'Neil, 2004a), along with diffusion-drag collisions (Men'shikov and Fedichev, 1995; Fedichev, 1997; Bass and Dubin, 2004). There is more discussion of these processes in Sect. VI.

C. Beyond Guiding Center Atoms

The theoretical studies of the three body $\overline{\mathrm{H}}$ formation and deexcitation have used a circular "guiding center atom" (GCA) model (Fig. 18(a)) (Glinsky and O'Neil, 1991; Men'shikov and Fedichev, 1995; Fedichev, 1997). Center-of-mass motion was allowed in a recent simulation (Robicheaux and Hanson, 2004) which still relies on the guiding center approximation. We now have the first indications of $\overline{\mathrm{H}}$ atoms that are too tightly bound to be treated with the guiding center approximation (Gabrielse *et al.*, 2004a).

For a GCA, the e^+ "guiding center" drifts around the $\bar{\mathrm{p}}$ with a drift velocity $\boldsymbol{v}_d = \boldsymbol{E} \times \boldsymbol{B}/B^2$ where the electric field is that of the $\bar{\mathrm{p}}$, and $\boldsymbol{B}$ is the strong field of the trap. This yields a circular orbit with angular drift or magnetron frequency $\omega_d = \omega_m = r_e c^2/(\omega_c \rho^3)$. Superimposed upon this drift motion is the much faster e^+ cyclotron motion at frequency ω_c, a motion with its own adiabatic invariant. Also superimposed is an axial oscillation of the e^+ back and forth along the direction of the magnetic field due to the restoring Coulomb force from the $\bar{\mathrm{p}}$, with angular oscillation frequency $\omega_z = \sqrt{r_e c^2/\rho^3}$ for small oscillation amplitude, and this motion too has its own adiabatic invariant.

Larger GCA orbits are in fact not circular because the center-of-mass and internal orbits of the $\overline{\mathrm{H}}$ are coupled (Vrinceanu *et al.*, 2004; Kuzmin and O'Neil, 2004a) but we will not discuss these complications here. Wave functions, spectra, and decay rates for high $|m|$ Rydberg atoms in a strong magnetic field have recently been calculated (Guest *et al.*, 2003; Guest and Raithel, 2003).

The regular cyclotron, axial and drift (i.e., magnetron) orbits are more akin to those of a particle in a Penning trap than to the familiar lower states of hydrogen, or even to the orbits of the Rydberg atoms that have been studied. The GCA model provides a useful and valid approximation when

$$\omega_d \ll \omega_z \ll \omega_c, \tag{7}$$

a condition that is very familiar for a charge in a Penning trap (Brown and Gabrielse, 1986).

Care must be taken in transforming this condition to a condition on atom size ρ because the frequencies vary so rapidly with ρ, and the circular GCA frequencies do not apply near GCA breakdown. We use the modest requirement that ω_d be at least three times smaller than ω_z, and that ω_z be at least three times smaller than ω_c. The circular GCA frequencies should then be reasonable estimates, allowing us to obtain the requirement that the GCA is valid only if the drift radius ρ is greater than ρ_3,

$$\rho > \rho_3 = \left[9 r_e c^2/\omega_c^2\right]^{1/3} = 0.14\ \mu\mathrm{m} \tag{8}$$

Here r_e is the classical electron radius and the specific value to the right is for ATRAP experimental conditions. Figure 18(d) shows that numerical calculations of internal $\overline{H}$ trajectories verify that GCA breaks down for atoms with size ρ smaller than this value. The slightly less stringent minimum ρ sometimes mentioned for GCA validity (Glinsky and O'Neil, 1991; Fedichev, 1997), which corresponds to all the circular GCA frequencies being equal, is the left vertical line in the Fig. 18(d).

ATRAP detects atoms which are smaller than ρ_3, and which are thus not appropriately described as GCA. The field ionization spectrum of Fig. 21 shows that some $\overline{H}$ atoms survive an analysis electric field $F_z = 360$ V/cm – the strongest analysis electric field we were able to produce in the current apparatus so far, given the need for stronger fields in the detection well. According to Eq. (6), such atoms have a radial size $\rho < 0.1$ μm. We have thus entered the regime where a GCA description of such atoms is not valid. $\overline{H}$ atoms of smaller radii might well be detected if larger F_z could be used.

$\overline{H}$ atoms beyond the reach of the GCA approximation are intriguing because for more tightly bound atoms it is generally assumed that the comparable strengths of the Coulomb and magnetic forces will result in chaotic trajectories (Kuzmin and O'Neil, 2004a). A technique must be found out to deexcite $\overline{H}$ atoms through the chaotic region to the more familiar, regular and manageable orbits and states that describe atoms of smaller size. Theoretical treatments of $\overline{H}$ formation and deexcitation which do not rely entirely upon the GCA are clearly needed.

D. First Measurement of the Speed of Slow $\overline{H}$ Atoms

As discussed earlier one of the two major challenges currently facing $\overline{H}$ research is to devise ways to produce $\overline{H}$ that is slow enough to trap. The required first step is to measure $\overline{H}$ velocities.

ATRAP recently measured the speed of some slow $\overline{H}$ atoms for the first time (Gabrielse *et al.*, 2004b). The pre-ionizing, analysis electric field represented in Fig. 17 is varied sinusoidally in time, and the number of $\overline{H}$ surviving this field is measured as a function of the oscillation frequency of the sinusoidally varying field (Fig. 22). The number drops as the frequency increases because less and less atoms are moving rapidly enough to pass through the ionization region while the electric field is small enough to not ionize them.

The expected decrease in the number of $\overline{H}$ that survive the oscillating field is shown by the solid curves in the figure for $\overline{H}$ atoms of several center-of-mass energies. For this first velocity measurement we measured the speed of the most weakly bound atoms in the distribution of Fig. 21. One could

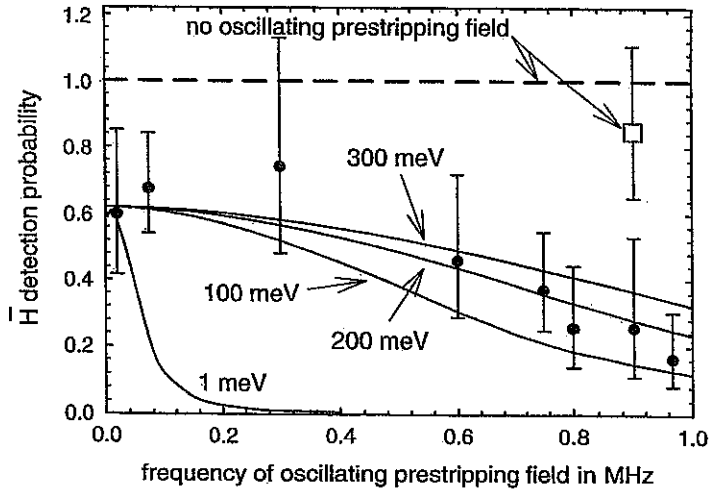

FIG. 22. The fraction of detected $\overline{H}$ atoms decreases as the frequency $\omega/(2\pi)$ of the oscillating electric field increases (solid points). More atoms are detected when there is no oscillating field (open square). This point is plotted on the same scale as the others but it has no frequency associated with it. The measured points are compared to a simple model discussed in the text; the solid curves apply when the oscillating electric field is applied, and the dashed curve when it is not. From (Gabrielse *et al.*, 2004b).

hope that these might have a velocity corresponding to the average thermal velocity they would have if they were at the temperature of the 4.2 K apparatus; instead their speed was about 30 times larger. Whether this is because we were simply driving the $\overline{p}$ too hard during the $\overline{H}$ production, or whether such a high velocity is characteristic of this method of $\overline{H}$ formation, is not yet known.

For a $\overline{p}$ traveling in the $\hat{z}$ direction through the e^+ plasma, one $\overline{p}$ speed that seems important is the one that equals the average axial speed of the e^+ that are moving in the same direction as the $\overline{p}$. For 4.2 K e^+ this corresponds to a $\overline{p}$ energy of 210 meV. This is close to what we measure, likely by coincidence given the approximate character of the estimate. One might expect increased $\overline{H}$ production at this $\overline{p}$ energy, but this depends in a complicated way upon how quickly the $\overline{p}$ are being cooled by the e^+. A recombination rate that depends upon the relative velocity of the $\overline{p}$ and e^+ will become insensitive to $\overline{p}$ energies below this value, since the relative velocity will be determined by the e^+ velocity.

Another important speed is

$$v_p = n_e(\pi b^2)v_e L. \tag{9}$$

This $\bar{p}$ speed would allow just enough time in the $L \approx 1$ mm thick e^+ plasma for there to be a deexcitation collision (Glinsky and O'Neil, 1991) between the e^+ initially picked up by the $\bar{p}$ and another e^+ in the plasma on average. The expected $e^+ - e^+$ collision rate should be of the order of $n_e(\pi b^2)v_e$ where $n_e = 1.6 \times 10^7/\text{cm}^3$ is the e^+ density and v_e is the average thermal speed for a e^+ at $T_e = 4.2$ K. The distance of closest approach b comes from equating the potential energy $(4\pi\varepsilon_0)^{-1}e^2/b$ and the thermal energy kT_e. The corresponding $\bar{p}$ energy, and hence the $\overline{H}$ energy, is around 400 meV – larger than what we observe. The cross section used is only an estimate, of course, and the e^+ may be some what heated by the $\bar{p}$. Notice that $v_p \propto n_e L T_e^{-3/2}$ suggesting that a e^+ plasma with a lower density, a shorter length and a higher temperature will produce $\overline{H}$ with lower velocities.

With both of these speeds being of the same order, and being closer to what we measure, it seems that most highly excited states are being formed about as rapidly as can be imagined, leaving no time for further cooling. By driving the $\bar{p}$ so that they have just enough energy to go through the e^+ plasma, it should be possible to make lower energy $\overline{H}$ atoms. In addition, it may be advantageous to keep the e^+ in a deep potential well so that weakly bound $\overline{H}$ will strip, giving the $\bar{p}$ further time to cool and to form more deeply bound states. For related reasons, it may also be advantageous to use an e^+ plasma that is very short along the direction of the magnetic field.

ATHENA measured the rate of $\overline{H}$ production as a function of elevated e^+ temperatures T during e^+ cooling of $\bar{p}$ in a nested Penning trap (Amoretti *et al.*, 2004). This measurement was interpreted as a test of the $\overline{H}$ production mechanism assuming that $\overline{H}$ was formed with $\bar{p}$ and e^+ in thermal equilibrium, with three-body $\overline{H}$ formation expected to have a $T^{-9/2}$ dependence, and radiative $\overline{H}$ formation a $T^{-1/2}$ dependence. The $\overline{H}$ production rate varied slowly with e^+ temperature, and production was observed even with room temperature e^+, with a rate too fast to be radiative recombination.

However, Eq. (9) suggests a non-equilibrium interpretation. The speed v_p corresponds to a $\bar{p}$ energy of about 1 keV, for $T = 15$ K, $L = 3.2$ cm and $n_e = 1.7 \times 10^8/\text{cm}^3$. (For higher temperatures v_p is lower.) Since this energy is larger than that of the $\bar{p}$ injected into the nested Penning trap, the highly excited $\overline{H}$ could form with velocities much higher than that of the e^+. The unusual observed temperature dependence then arises because three-body formation (Eq. (1)) is so rapid that the assumed thermal equilibrium does not apply. With this interpretation very high speed $\overline{H}$ atoms indeed were produced by ATHENA.

A very recent simulation supports this interpretation (Robicheaux and Hanson, 2004; Robicheaux, 2004) for the simplest application of e^+ cooling of $\bar{p}$ used in ATRAP and ATHENA's first $\overline{H}$ observations, and in all subsequent ATHENA experiments. The variation subsequently used by ATRAP, discussed in Sect. IV.C. and in (Gabrielse *et al.*, 2002b), cannot be easily simulated. In this method a radio frequency drive is used to gently excite the $\bar{p}$ into contact with the e^+. The speed of the $\bar{p}$, and hence the $\overline{H}$ that form, is thus determined by the strength and frequency of the drive.

As mentioned above, our method of driving the e^+ cooling of $\bar{p}$ should produce much slower $\overline{H}$ atoms once this drive frequency and amplitude are carefully adjusted. For atoms that are moving much slower than those we have observed so far, more care will be needed to extract the $\overline{H}$ velocity from the oscillating field measurements described above. The $\overline{H}$ travels through a large electric field gradient as it enters the detection trap, and the force on the highly polarizable $\overline{H}^*$ (Vrinceanu *et al.*, 2004; Kuzmin and O'Neil, 2004c) modifies the $\overline{H}$ trajectory. We showed that the force was too small to substantially modify the motion of the 200 meV $\overline{H}$ atoms we observed (Gabrielse *et al.*, 2004b) (using the polarizability that we had calculated for circular GCA atoms (Vrinceanu *et al.*, 2004) to calculate $\overline{H}$ center-of-mass motion) but warned that this would not be so for atoms that move a lot more slowly. A more recent calculation (Kuzmin and O'Neil, 2004b) shows that slow $\overline{H}$ atoms that are created off the center axis of our trap, when polarized by radial electric fields, can even follow radially diverging trajectories that could keep them from reaching our detection well and being counted.

E. Deexcitation of Highly Excited States

Three body $\overline{H}$ formation produces large numbers of guiding center $\overline{H}$ atoms. Ground state $\overline{H}$ atoms are desired. The deexcitation of highly excite $\overline{H}$ atoms is crucial, and several different methods have been mentioned.

(1) Collisional deexcitation of the $\overline{H}$ within an e^+ plasma is discussed in Sect. V.C.

(2) The lifetimes of excited $\overline{H}$ states are typically very long. They are shorter for more tightly bound states. A state with principal quantum number $n \lesssim 15$ will rapidly deexcite to the ground state via radiation. Collisions with e^+ in the plasma will change the angular momenta so the states will more quickly radiate. Radiative decays of Rydberg states have recently been considered (Flannery and Vrinceanu, 2003; Guest *et al.*, 2003).

(3) Laser stimulated deexcitation is challenging because three body formation produces states with binding energies spread over a very wide range compared to the energy spread of typical laser photons, and because the spatial overlap of the highly excited states and the desired lower states seems to be very small. A first theoretical look at this is in a very recent simulation (Robicheaux and Hanson, 2004).
(4) The use of sequences of half-cycle laser pulses has recently been considered (Hu and Collins, 2004).
(5) Given the similarity of GCA states and circular Rydberg states, it may be possible to use adiabatic fast passage to deexcite atoms.

VI. Three Body $\overline{H}$ Formation, and Related Experiments

There was much excitement and some concern when we realized many years ago (Gabrielse *et al.*, 1988) that the likely $\overline{H}$ formation mechanism for very cold plasmas of e^+ and $\bar{p}$ was the three body process

$$\bar{p} + e^+ + e^+ \longrightarrow \overline{H}^* + e^+. \tag{10}$$

The excitement was because simple arguments suggested that the rate for this process would vary as $T^{-9/2}$. This would make an enormous rate if this scaling was valid at 4 K. I often said that this process would be either the high rate $\overline{H}$ signal (if we found a way to use it to produce useful $\overline{H}$) or the noise we would need to avoid (if we preferred another formation process) since no other $\overline{H}$ formation process could come within orders of magnitude of competing with this rate.

One concern arose because using this formation mechanism at low temperatures had never been considered before. The matter counterpart of this process had been studied, but only for the much higher temperatures of interest for astrophysical applications (Bates *et al.*, 1962; Makin and Keck, 1963; Stevefelt *et al.*, 1975). The second major concern was about the role of the magnetic and electric fields in the nested Penning trap (Gabrielse *et al.*, 1988) that we had proposed as a way of realizing $\overline{H}$ formation. How would they modify the $\overline{H}$ production rate? It seemed that magnetic field might not change the density of states and the rate too much, but a proper calculation was needed. The third concern was that the matter counterpart of this process had been studied for infinitely extended plasmas and infinite time scales, while we could only manage rather small plasmas in a trap interacting for not such long time scales. How quickly would $\overline{H}$ formed in highly excited states be deexcited to the ground states that we needed for our $\overline{H}$ trapping and spectroscopy?

Several theoretical groups took up these challenges. First, a quantum calculation suggested that the scaling was indeed valid all the way down to 4 K if no magnetic field was present (Zygelman and Dalgarno, 1989). An extended version of this work was reported much later (Zygelman, 2003).

The magnetic field challenge was then taken on (Glinsky and O'Neil, 1991). The guiding center atom (discussed in Sect. V.C) was introduced as a method of dealing with highly excited states in a strong magnetic field. The encouraging conclusion was the $T^{-9/2}$ scaling would hold down to 4 K even in a strong magnetic field. Moreover, the strong field would only decrease the rate by a factor of ten for the same temperature compared to what was calculated for no magnetic field. Replacement collisions were essential in maintaining the high rate. A free e^+ would be captured on a field line closer to the $\bar{p}$, than the e^+ that had been bound to the $\bar{p}$ on a field line farther away. However, the simulations suggested that that deexcitation to a low state might be a problem with finite interaction times and volume for the $\bar{p}$ and e^+. Interrupted three body formation and deexcitation would yield highly excited GCA.

The simulation illustrates quite well general features of three body $\overline{H}$ formation in a strong magnetic field, but is not able to yet predict the distribution of excited states that can be measured. In Sect. V.C we discuss a suggestion that our ATRAP field ionization spectrum (Gabrielse *et al.*, 2002b) could be accounted for by comparing our data to the tails of the numerical simulations (Glinsky and O'Neil, 1991). While we wish that this claim was true, Sect. V.C also reviews why we think that such comparisons are still premature (Gabrielse *et al.*, 2004).

A later analytic treatment did not include replacement collisions and thus reached a more pessimistic conclusion about the $\overline{H}$ formation rate (Men'shikov and Fedichev, 1995). However this work did include the $\overline{H}$ deexcitation caused by many gentle, long range collisions of the $\overline{H}$ and e^+ in the cold plasma – diffusion drag collisions – that were not included in (Glinsky and O'Neil, 1991). One of the authors then treated three body formation and deexcitation using both the replacement collisions which would initially dexcite $\overline{H}$ atoms, and the diffusion-drag collisions which then would take over for smaller $\overline{H}$ radii (Fedichev, 1997). According to this work, deexcitation would proceed very rapidly in the diffusion-drag regime. This apparently was too good to be true. A recent treatment suggests that an adiabatic invariant will prevent the diffusion-drag deexcitation process from carrying the deexcitation to much smaller radii than did the replacement collisions (Bass and Dubin, 2004).

The GCA (Glinsky and O'Neil, 1991) remains an important starting point for any discussion of three body formation in a strong magnetic

field, since it is such highly excited states that are readily formed in the experiments. This model can be extended to include the unavoidable coupling between the internal motion of an excited $\overline{H}$ and the center-of-mass motion of the $\overline{H}$ (Vrinceanu *et al.*, 2004; Kuzmin and O'Neil, 2004a) caused by the magnetic field. A conserved pseudo momentum makes it possible to make an effective potential for the internal motion of a e^+ orbit within an $\overline{H}$ atom in which the coupling to center-of-mass motion takes the form of a small harmonic offset potential for the e^+. For states that are more deeply bound this coupling and offset is less important. The polarization and ionization of highly excited $\overline{H}$ has been discussed (Vrinceanu *et al.*, 2004), and very recently the motion of GCA in electric and magnetic fields has been considered (Kuzmin and O'Neil, 2004b).

A very recent simulation of three body of $\overline{H}$ formation (Robicheaux and Hanson, 2004) still makes use of the guiding center approximation but does include the coupling between the center-of-mass motion and the internal motion of the $\overline{H}$. The recombination rate for a 5.4 Tesla field is 60% larger than for $B \rightarrow \infty$ in the earlier simulation (Glinsky and O'Neil, 1991) – whether this is because of a different magnetic field or because of the center-of-mass coupling is not clear. An extension of this calculation (Robicheaux, 2004) attempts the daunting challenge of more realistically modeling the environment of a nested Penning trap. Qualitatively consistent with the observations and discussion in (Gabrielse *et al.*, 2004b) and in Sect. V.D, the simulation shows $\overline{H}$ form before the $\bar{p}$ have completely cooled, and also suggests that a shorter e^+ plasma produces slower $\overline{H}$ atoms. Limited statistics prevent making quantitative comparisons with measured field ionization spectrum (e.g., Fig. 21 discussed in Sect. V.A) especially for the most deeply bound states, but this may become possible.

An important message of Sect. V.C is that more extensive simulations over a wider range of $\overline{H}$ binding energies are required if there is to be a meaningful comparison of theory and experiment. These should include replacement collisions and diffusion-drag collisions. They should also include the unavoidable coupling of the center-of-mass and the internal orbits of the $\overline{H}$. Finally, the methods used must work not only for circular GCA states, but also for more tightly bound states which cannot be described as GCA, and whose orbits are expected to be chaotic.

Three body formation of other Rydberg atoms has been observed and is being studied for ion-electron plasmas produced by laser ionization just above threshold (Kilian *et al.*, 1999, 2001; Roberts *et al.*, 2004; Simien *et al.*, 2004). A major difference is the absence of the strong magnetic field.

VII. Production Method II: Laser-Controlled $\overline{H}$ Production

We are quite excited about our ATRAP demonstration of a new method to produce slow antihydrogen, in which lasers control the $\overline{H}$ formation (Speck *et al.*, 2004; Storry *et al.*, 2004).

$\overline{H}$ formation via the collisions of ground state *Ps* and trapped $\bar{p}$ was proposed long ago (Humberston *et al.*, 1987), and the counterpart process in which a proton is substituted for a $\bar{p}$ has been used to produce hydrogen (Merrison *et al.*, 1997). However, the observed rate was slow and fewer $\bar{p}$ than protons are available, so no attempt has been made to form $\overline{H}$ by this method.

The cross section and $\overline{H}$ formation rate from collisions of highly excited Rydberg Ps^* with $\bar{p}$ are enormously larger. The use of laser-excited *Ps* was thus proposed (Charlton, 1990) but never realized. We recently demonstrated (Speck *et al.*, 2004) the alternative of producing Ps^* by laser controlled charge exchange (Hessels *et al.*, 1998). These Ps^* then collide with trapped $\bar{p}$ to form $\overline{H}^*$ (Storry *et al.*, 2004).

The three steps of this process were listed in the Introduction and Overview, in Eqs. (2–4), and Fig. 23 gives a schematic overview of how these steps are realized. Three coaxial Penning traps (yellow regions) are arranged so that they are as close together as possible. In preparation for laser-controlled $\overline{H}$ production, 4.2 K e^+ are located in the first of these (left). Cold $\bar{p}$ are located in the adjacent trap (center). The detection trap (right) is initially empty. Two lasers excite a *Cs* beam so that Cs^* travel perpendicular to the axis of the traps and through the trapped e^+ to produce highly excited Ps^* via a resonant charge change collision. Some of the Ps^* travel through the trapped $\bar{p}$ and are able to produce $\overline{H}^*$ via a second resonant charge exchange collision. A small fraction of the $\overline{H}^*$ enters the detection trap and is ionized by the electric field within it. The $\overline{H}^*$ deposits its $\bar{p}$ in the detection trap for later counting.

Figure 24 shows evidence that in this demonstration about 16 $\overline{H}$ were ionized in the detection well. However, if the $\overline{H}$ production is isotropic then these events signal the production of about 200 $\overline{H}$ atoms. The $\overline{H}$ formed would naturally seem to have the low temperature of the trapped $\bar{p}$, though this has yet to be demonstrated. This proof-of-principle experiment was carried out at the end of the 2003 $\bar{p}$ run at the CERN AD, with only several hours of trials. More $\overline{H}$ production is expected as the method is refined and optimized.

The strong 5.3 T magnetic field is an essential part of the three traps, but it also complicates this experiment and its theoretical interpretation. First, exciting the Cs atoms from the $6P_{3/2}$ state to the Rydberg state requires

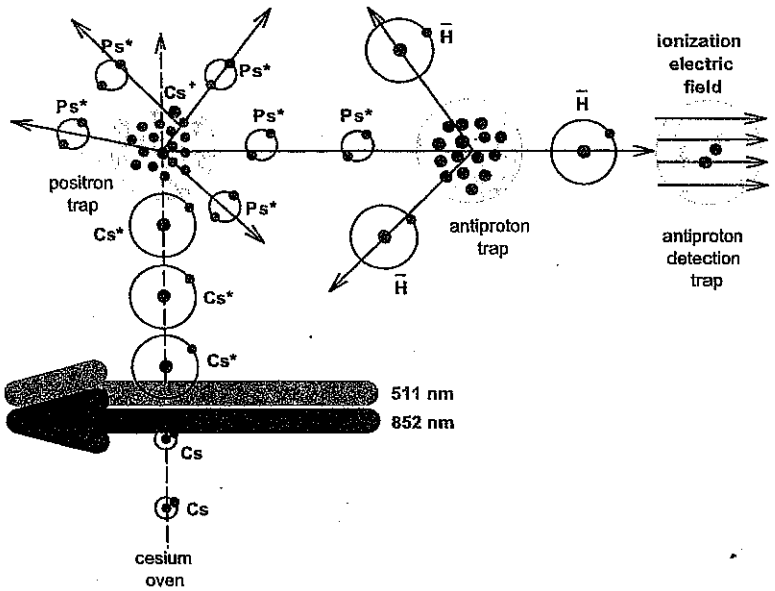

FIG. 23. Basic scheme for laser-controlled production of cold antihydrogen. From (Storry *et al.*, 2004).

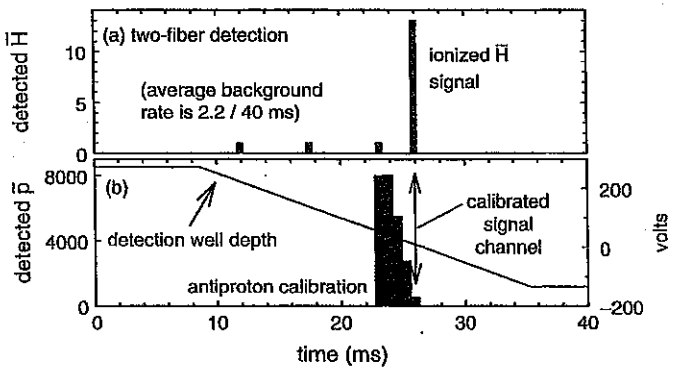

FIG. 24. (a) $\overline{H}$ detected (peak) as the potential well containing the ionized $\overline{H}$ is ramped down. (b) $\bar{p}$ annihilation signal as the axial well depth is reduced through zero. From (Storry *et al.*, 2004).

empirically varying an electric field to tune the atoms into resonance with the fixed frequency copper vapor laser since the states have not been calculated. Second, internal orbits of both the Cs^* and $\overline{H}^*$ atoms formed are significantly modified by B since the magnetic force is comparable to the

Coulomb force. Third, the binding energies of Rydberg atoms moving across a strong magnetic field are not even conserved, but are instead coupled to the center of mass energy of the atoms (Vrinceanu *et al.*, 2004; Kuzmin and O'Neil, 2004a). A calculation of this double charge exchange process which neglects the magnetic field (Hessels *et al.*, 1998) gives a guide about what to expect, but a formation calculation that includes the crucial role of the magnetic field is needed.

VIII. Comparing the $\overline{H}$ Production Methods

Which of the two demonstrated $\overline{H}$ production methods is more useful in producing extremely cold, ground state $\overline{H}$ that can be trapped for precise spectroscopic comparisons with hydrogen and for gravitational studies? It seems to early to tell.

Laser-controlled charge exchange has the advantages of naturally producing both colder atoms and a much narrower, laser-selected distribution of excited states. However, a method to deexcite them to the ground state has yet to be demonstrated.

$\overline{H}$ produced during e^+ cooling of $\bar{p}$ in a nested Penning trap produces atoms more easily and at a much higher rate, and it may be possible to collisionally deexcite them. However, now that the velocity of these $\overline{H}^*$ can be measured (Gabrielse *et al.*, 2004b), it remains to be seen if ATRAP's method for driving $\overline{H}$ production (Gabrielse *et al.*, 2002b) or some variant can produce very cold atoms as hoped.

Other production methods, like using a CO_2 laser to stimulate $\overline{H}$ formation in a trap (Gabrielse *et al.*, 1988; Wolf, 1993), have yet to be experimented with. The best method for producing useful $\overline{H}$ is not yet clear.

IX. Future

A. Antihydrogen Trapping

A.1. Can ground state antihydrogen and its ingredients be trapped together?

A long term goal of slow antihydrogen experiments, quoted in the Introduction and Overview, is to trap ground state $\overline{H}$ atoms for precise spectroscopy experiments (Gabrielse, 1987). When these goals were laid out long ago the first atoms had only recently been trapped (Migdall *et al.*, 1985), and a proposal to trap spin polarized hydrogen atoms was just appearing (Hess, 1986). It is very encouraging that hydrogen atoms were

subsequently trapped (Hess *et al.*, 1987; Roijen *et al.*, 1988), laser cooled (Setija *et al.*, 1993) and used for precise hydrogen spectroscopy (Cesar *et al.*, 1996).

The simplest way to load $\overline{H}$ into such a trap would be if the cold $\overline{H}$ atoms would be created directly within the trap, and thus be trapped as soon as they are created. A great concern is that the e^+ and $\overline{p}$ might be lost from their respective traps before $\overline{H}$ forms, for traps which break the axial symmetry of a Penning trap, as is the case if a Ioffe trap field is added to a Penning trap. The stability of charges in a Penning trap is closely related to axial symmetry; the resulting conservation of angular momentum gives rise to a confinement theorem (O'Neil, 1980). Neither a charged particle nor a dense single-component plasma, can spread perpendicularly to the magnetic field enough to leave a Penning or Malmberg trap. Breaking the axial symmetry voids the confinement theorem.

An experimental realization of a Penning-Ioffe trap configuration (Fig. 25(a)) could direct the magnetic field of a solenoid (not pictured) along the axis of the stacked rings of an open-access Penning trap (Gabrielse *et al.*, 1989c). The Ioffe field would come from currents through vertical Ioffe bars and through "pinch coils" above and below, or magnetic materials arranged to give the same field configuration.

For simplicity of our analysis, we assume that the "pinch coils" are away from the central region where charged particles would be trapped. The addition of the radial magnetic quadrupole field of a Ioffe trap to the field $B_0\hat{z}$ for the Penning trap,

$$\vec{B} = B_0[\hat{z} + (x\hat{x} - y\hat{y})/R], \tag{11}$$

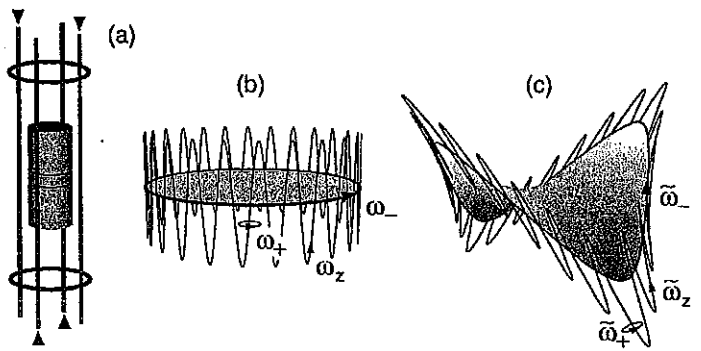

FIG. 25. (a) Open access Penning trap electrodes, with vertical current bars and pinch coils of a Ioffe trap. Orbits for a charged particle in a Penning trap (b) without and (c) with a radial Ioffe field. From (Squires *et al.*, 2001).

then destroys the axial symmetry about $\hat{z}$, and introduces a distance scale, R. Axial symmetry, present for large R, is destroyed as R is reduced (e.g., by increasing the Ioffe current). Superconducting coils could produce a Ioffe gradient, $C_1 = B_0/R$, as large as 40 T/m, even for a bias field $B_0 = 2$ T, whereupon $R = 5$ cm. The well depth energy (written in terms of an effective temperature depth T) for a Bohr magneton μ_B within a trap of radial size ρ is

$$kT = B_0\left[\sqrt{1+\left(\frac{\rho}{R}\right)^2}\right] \approx \frac{\mu_B B_0}{2}\left(\frac{\rho}{R}\right)^2. \tag{12}$$

A trap with the parameters mentioned above, at a radius $\rho = 2$ cm, would have a well depth that corresponds to 0.1 K.

To investigate the breakdown of stable confinement (after trying in vain to interest real theorists in solving this problem for a number of years) we examined the motion of a charge in a Penning trap with a radial Ioffe magnetic field using a guiding-center approximation (Lehnert, 1964), a perturbation expansion using the method of multiple time scales (Bender and Orszag, 1978), and exact numerical calculations. At roughly the same time, experiments and analysis were underway for such a field superimposed upon a Malmberg trap (Gilson and Fajans, 1999).

We found stable orbits and largely separated motions that are associated with adiabatic invariants (Squires *et al.*, 2001). Figure 25(b) shows the familiar orbit of a charge in a Penning trap, and Fig. 25(c) shows how this orbit changes when the radial field of a Ioffe trap is added. The basic orbit can be understood as motion along a force-free sheet that also conserves energy, Fig. 26. Resonant instabilities arise when the period of the modified

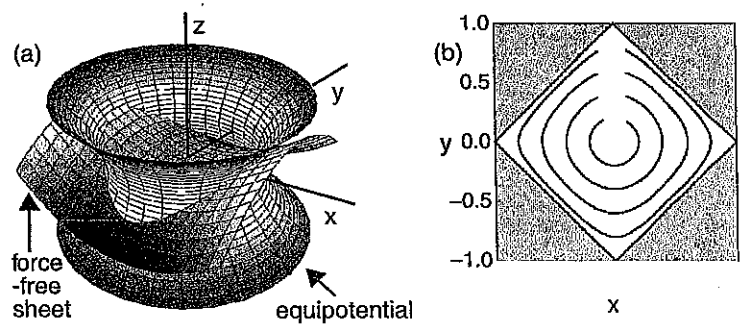

FIG. 26. (a) The force-free sheet and an equipotential of the electrostatic quadrupole. (b) Projections of stable magnetron orbits upon the xy plane lie within a square. From (Squires *et al.*, 2001).

magnetron motion (sometimes called $\boldsymbol{E}\times\boldsymbol{B}$ drift motion) is an integer multiple of the axial oscillation period. However, we concluded that these resonances can be avoided at least for low particle densities.

The stable motion of a single charge in a Penning-Ioffe trap made us cautiously optimistic that this configuration might work as long as the density of charges was low enough. Collisions are notoriously effective in breaking adiabatic invariants, and adiabatic invariants are crucial for the stable orbits that we observed. It thus seemed clear that there would be stability problems above some density.

What density might this be? We do not know. The natural density to use seems to be the number of charged particles in a volume that is the cube of the Debye screening length for a charge in the plasma, $n\lambda_D^3$. Here the number density of the particles is n, and the Debye screening length for a charge e in a single component plasma at temperature T is

$$\lambda_D = \sqrt{\frac{\epsilon_0 kT}{ne^2}} \tag{13}$$

in SI units. For typical ATRAP parameters $n = 1.6\times10^7/\mathrm{cm}^3$ and $T = 4.2$ K, there are only 0.25 charged particles per Debye volume. Unfortunately, we do not know at what natural density the low density analysis will break down in this regime in which $n\lambda_D^3 < 1$.

Our proposal and analysis (Squires *et al.*, 2001) provoked a rather direct response two years later based on extrapolating an experiment done in a Malmberg–Penning trap to ATRAP Penning–Ioffe conditions, in which case it is said to "contradict" our conclusion (Gilson and Fajans, 2003). What is an issue is the applicability of our one-particle analysis (which is not disputed) to the case of more than one trapped particle. Below what particle density can the resonances (that both groups had carefully considered) be avoided? Is density alone the relevant indicator of where the single particle analysis can no longer be applied to, and if so at what density?

The experiment that showed significant radial transport of charged particles was done in a Malmberg–Ioffe trap using much smaller fields and gradients than we had in mind, and much hotter plasmas. Typical conditions $B_0 = 0.021$ T and $C1 = 0.0002$ T/m, for example, correspond to an extremely large $R = 100$ m. The particle density $n = 10^7/\mathrm{cm}^3$ is almost the same as at ATRAP, but the temperature $T = 12000\ K = 1$ eV is 3000 times higher than ATRAP's cryogenic temperature.

To extrapolate to the ATRAP high field and low temperature conditions seems like quite a stretch, for three reasons. First, the natural density for the first experiment is $n\lambda_D = 4.6\times10^4$. This is more than five orders of magnitude larger than what was considered above, and goes between the

cases $n\lambda_D^3 \gg 1$ and $n\lambda_D^3 < 1$. Second, the trap field and gradient require that R also be extrapolated by a large factor, of about 2000, indicating much stronger axial symmetry breaking under ATRAP experimental conditions. Third, the very long plasma column in the Malmberg trap seems likely to have broader resonances, and a somewhat different charged particle transport, compared to the smaller and more spherical e^+ plasmas in a Penning trap that ATRAP utilizes.

At ATRAP we are encouraged by recently observing that trapped electrons survive a radial Ioffe gradient for hours – much longer than needed to accumulate $\bar{p}$ and form $\overline{H}$. The radial field of a Ioffe trap, from a permanent magnet apparatus constructed by our Jülich collaborators, was added to the ATRAP Penning trap. For a bias field $B = 3$ T, the magnets were able to maintain $C_1 = 16$ T/m, which corresponds to $R = 19$ cm. This R is larger than what we eventually hope to achieve, but still very much smaller than for the low field experiment discussed earlier. Such investigations are still underway, with much remaining to be studied.

A.2. Proposed trapping alternatives

Several suggestions have been made for trap geometries (for charge particles and neutral atoms) that are axially symmetric, or have less asymmetry than the Penning–Ioffe configuration. Three axially symmetric suggestions (Dubin, 2001) seem very challenging experimentally. Higher order magnetic traps would reduce the size of the magnetic gradient over most of the trapping volume (Fajans and Schmidt, 2004), but would confine atoms in a larger volume than can likely be illuminated by spectroscopy lasers. A magnetic cusp trap has also been proposed (Mohri and Yamazaki, 2003).

A.3. Trapping excited antihydrogen states?

The $\overline{H}$ trapping discussed here is for an $\overline{H}$ atom in its ground state. We are intrigued by the possibility that the highly polarizable GCA states created in large numbers during e^+ cooling of $\bar{p}$ could be trapped in electric field gradients (Gabrielse *et al.*, 2002a) for the time needed to deexcite them to the desired low excitation states. Perhaps this could be done using the electrostatic quadrupole of a Penning trap. What is needed is enough trapping time for deexciting the $\overline{H}$ down to states with principal quantum numbers $n \sim 15$ which then deexcite rapidly to the ground state by radiation. The polarization of GCA states and the resulting fields required for confinement have been discussed (Vrinceanu *et al.*, 2004). However, these elements have not yet been put together to make a workable solution for free $\overline{H}$ atoms.

More recent theory provides more information about the polarizability and motion of a GCA in electric and magnetic fields (Kuzmin and O'Neil, 2004b), and explores the possibility of two and three dimensional trapping of polarizable $\overline{H}$ GCA within the electric field produced by a dense e^+ plasma.

B. Will Collisions with Matter Atoms Cool or Annihilate $\overline{H}$ Atoms?

B.1. Cooling $\overline{H}$ via collisions with hydrogen atoms?

Is it possible to cool $\overline{H}$ atoms by simply introducing hydrogen atoms into the vacuum system that contains them? There is no answer to this question for the highly excited states that have been produced and identified so far – though the larger size of these atoms will make larger cross sections. However, a lot of recent theoretical work has focussed upon collisions of ground state $\overline{H}$ and H atoms since this was first discussed many years ago (Shlyapnikov *et al.*, 1993).

The elastic scattering channel that provides the cooling (Froelich *et al.*, 2000; Jonsell *et al.*, 2001) must be compared to several inelastic channels by which $\overline{H}$ atoms are lost.

$$\text{Rearrangement}: H + \overline{H} \longrightarrow p\overline{p} + e^+e^- \tag{14}$$

$$\text{Direct}: H + \overline{H} \longrightarrow p\overline{p} + e^+ + e^- + \text{annihilationproducts} \tag{15}$$

$$\text{Lepton}: H + \overline{H} \longrightarrow p + \overline{p} + \text{photons} \tag{16}$$

$$\text{RadiativeAssociation}: H + \overline{H} \longrightarrow H\overline{H} + h\nu \tag{17}$$

The losses come from a rearrangement channel in Eq. (14) and a direct annihilation channel in Eq. (15) (Froelich *et al.*, 2000; Jonsell et al., 2000, 2001; Armour and Chamberlain, 2002; Armour *et al.*, 2004). Interestingly, when $\overline{H}$ and H collide, the annihilation of the e^+ and the electron in Eq. (16) takes place at a much smaller rate (Froelich, 2002; Froelich *et al.*, 2004a). The radiative association process is notable for the unusual quasi-bound $H\overline{H}$ states that may be produced (Zygelman *et al.*, 2001; Froelich *et al.*, 2004b) rather than for making a substantial contribution to the inelastic cross section.

Early estimates of cross sections had led to the conclusion that cooling to 0.1 K might be possible with a loss of 90% of the atoms (Froelich *et al.*, 2000; Jonsell *et al.*, 2001; Dalgarno *et al.*, 2001). Improved calculations that include the rearrangement channel (but not the direct annihilation channel) lead to the conclusion that cooling to only 0.43 K results in 90% atom loss

(Armour and Chamberlain, 2002; Zygelman *et al.*, 2004; Voronin and Carbonell, 2004). Putting the latest rearrangement (Zygelman *et al.*, 2004) and direct annihilation (Jonsell *et al.*, 2004b) cross sections together now seems likely to push this critical temperature to 1 K or above (Jonsell, 2004), though there are still uncertainties in the rearrangement cross section to be addressed (Zygelman *et al.*, 2004). A strong interaction potential is being used to calculate $\overline{p}$ annihilation in the elastic channel (Armour, 2004a).

The possibility to use H atoms to cool $\overline{H}$ depends in a critical way upon the temperature dependent ratio of elastic and inelastic cross sections. A superconducting Ioffe trap will likely be not deeper than 0.5 K when a strong bias field is present, so cooling without annihilation to well below this temperature is required if such collisional cooling is to be practical.

There are now plans to calculate $\overline{p}$ annihilation in the elastic channel of collisions of $\overline{H}$ with hydrogen molecules (Armour, 2004b).

B.2. Cooling $\overline{H}$ via collisions with he atoms?

Can collisions with He gas be used to cool ground state $\overline{H}$ atoms? (Collisions with highly excited $\overline{H}^*$ should also be considered.)

Different nuclear charges produces interesting differences between $\overline{H}$ collisions with helium and hydrogen (Armour and Chamberlain, 2001). Born–Oppenheimer potentials for the $\overline{H}$–He system are available (Strasburger and Chojnacki, 2002), and a large effort is currently underway to calculate the cross sections for all of the various channels (Jonsell *et al.*, 2004a; Armour, 2004a). A calculation of the elastic scattering (Sinha and Ghosh, 2003) neglects the strong interaction which, however, seems to substantially modify the elastic scattering (Jonsell *et al.*, 2004a). The production of He–$\overline{p}$ and α–$\overline{p}$ is being investigated (Todd *et al.*, 2004)

Unfortunately, the annihilation rate in the elastic channel already seems to be much higher for $\overline{H}$ collisions with He compared to collisions with hydrogen atoms, making it unlikely that He will be useful for cooling $\overline{H}$ atoms.

B.3. Collisions, annihilation and vacuum

The observed $\overline{p}$ lifetime was used many years ago to estimate that the background pressure in the cryogenic system in which store $\overline{p}$ was better than 5×10^{-17} Torr (Gabrielse *et al.*, 1990) – about a million times smaller pressure than can be measured with good commercial gauges. The most likely contaminants gas in a cryogenic system is helium, with hydrogen and probably hydrogen molecules of some interest as well.

The collision calculations reviewed above, when finished and taken together, should make it possible to use the observed lifetime of trapped $\overline{H}$

as a measure of the pressure of background pressures of helium and other gasses. What is needed, for example, is an $\overline{H}$ lifetime as a function of the $\overline{H}$ energy and the helium density, for helium gas in thermal equilibrium at temperatures ranging from 0.1 to 4.2 to 15 K. The same could be done for $\overline{H}$–H. Ideally these graphs would be contrasted to those for $\overline{p}$–He and $\overline{p}$–H, for $\overline{p}$ at rest. The cryopumping of helium to surfaces can be folded in separately as appropriate for particular vacuum systems.

C. Continuous Lyman Alpha Source

Extremely accurate measurements of frequency of the 1s–2s transition in antihydrogen should provide the most accurate possible comparison of the simplest atoms of antimatter and matter. Spectroscopy of the $\overline{H}$ 1s–2p might be an interesting place to begin with, and two-photon spectroscopy with the first of the photons being closer to the 1s–2p transition frequency would follow naturally. All of these spectroscopy examples require a source of Lyman alpha photons at 121.5 nm – for either the spectroscopy itself or for cooling of the atoms that is required to get a high precision.

For this purpose, the ATRAP collaborators from Garching have built and demonstrated the first continuous source of Lyman alpha radiation (Eikema *et al.*, 1999), at 121.5 nm. A representation of the 4-wave mixing apparatus is in Fig. 27. This source was then used to observe 1s–2p transitions with a linewidth that was very close to the natural linewidth for these transitions (Eikema *et al.*, 2001), as illustrated in Fig. 28. Up to 20 nW of power was reported (enough for spectroscopy and some laser cooling),

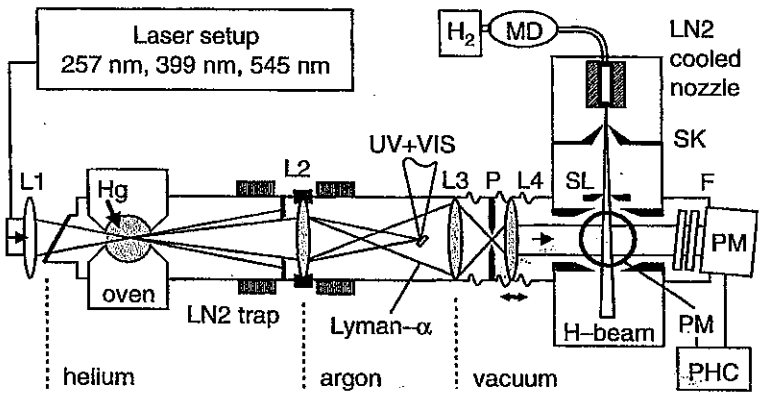

FIG. 27. Apparatus used to generate the first continuous coherent Lyman alpha radiation by sum-frequency mixing in mercury vapor. From (Eikema *et al.*, 2001).

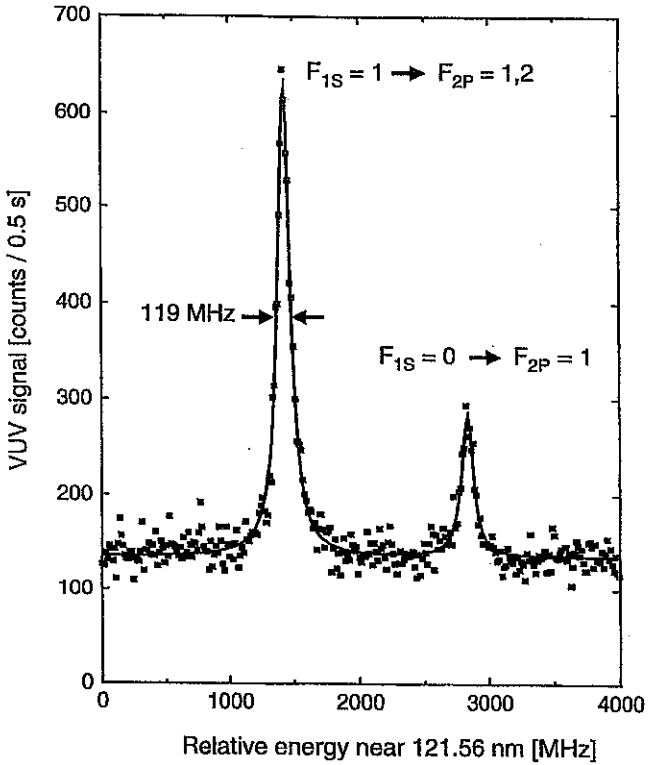

FIG. 28. Hydrogen 1s–2p resonances lines observed using the continuous Lyman alpha radiation source. From (Eikema *et al.*, 2001).

with a beam quality that allows the photons to pass through a 0.5 mm pinhole.

X. Conclusions

In an exciting three years, slow antihydrogen has been produced by two different production methods. In method I, $\overline{H}$ is produced during positron cooling of antiprotons in a nested Penning trap. In method II, lasers control the $\overline{H}$ production for the first time. The experiments all use the techniques our TRAP collaboration developed to accumulate cold antiprotons, at an energy that is 10^{10} times lower than $\overline{p}$ circulating in any storage ring. The $\overline{H}$ experiments are all being carried out at a storage ring that was specially constructed to make these experiments possible.

Most of the slow antihydrogen has been produced during positron cooling of antiproton in a nested Penning trap. Our TRAP and ATRAP collaborations developed this device and technique for this purpose over many years – first with electrons and protons, and then with positrons and antiprotons. For their first observations of slow antihydrogen, both ATRAP and ATHENA used the most straight forward, one-time positron cooling of antiprotons in a nested trap. To count the atoms, ATRAP used field ionization detection, and ATHENA used $\overline{H}$ annihilation detection.

ATRAP then moved to a variation on the positron cooling production method by driving the antihydrogen production so that there are many cycles of positron cooling in the nested Penning trap. The first advantage of this variation is that more antihydrogen is produced. The second advantage is that it should be possible to give the $\bar{p}$ the minimum energy needed to contact the positrons if the drive amplitude and frequency are optimized, which has not yet been done.

ATRAP's field ionization method shows that it is highly excited antihydrogen atoms that are being made in large numbers. The field ionization method also makes it possible to go beyond $\overline{H}$ counting to make progress on two crucial challenges now facing slow antihydrogen research.

The first crucial challenge is to deexcite the highly excited atoms that are being produced in large numbers down to the ground state. The field ionization technique provides the only way to detect which states are produced, information that is needed if the production parameters are to be optimized for the production of the most deeply bound states.

The second crucial challenge is to produce $\overline{H}$ atoms with a velocity that is low enough that such particles could be trapped for precise spectroscopy experiments. A variation of ATRAP's field ionization detection, with an oscillating analysis electric field, makes it possible to measure an $\overline{H}$ velocity for the first time. An $\overline{H}$ velocity substantially above the average thermal velocity for a 4 K ambient temperature was observed in the first demonstration. However, there is hope that optimizing the driven $\overline{H}$ production during positron cooling in a nested Penning trap will result in lower velocities.

ATRAP has recently demonstrated a second, entirely different method to produce cold antihydrogen – the first laser-controlled $\overline{H}$ production mechanism. Laser frequencies determine the $\overline{H}$ binding energy. This method seems to naturally produce $\overline{H}$ atoms with the energy distribution of the $\bar{p}$ from which they form. It seems possible with techniques demonstrated with electrons to make this energy very low.

An interesting possibility is to capturing cold $\overline{H}$ atoms as they are produced, within a neutral particle trap. There is currently some controversy about whether the e^+ and $\bar{p}$ can remain trapped at the same time, when the

fields of a Ioffe trap are added to confine $\overline{H}$ atoms. It is thus encouraging that trapped electrons seems to survive such a field for substantial times, but much yet be studied here.

A great deal remains to be done before accurate spectroscopic comparisons of antihydrogen and hydrogen can begin. However, the regular production of slow antihydrogen atoms is a big step forward – even though none of these atoms has yet been shown to be useful for precise spectroscopy in a trap. A great deal has been accomplished – enough to give hope for continued progress at a similar rate.

XI. Acknowledgments

It has been and remains an honor and pleasure to lead the ATRAP collaboration, as it was the TRAP collaboration from which it grew. The ATRAP team (table I) is very dedicated and skilled, as is needed for such demanding experiments. Special thanks to ATRAP members for their comments on this review – especially to A. Speck, C. Storry, E.A. Hessels, W. Oelert and J. Walz. Thanks for helpful discussions and comments to E.A.G. Armour, J. Fajans, P. Froelich, S. Jonsell, T. O'Neil, and B. Zygelman.

I am grateful to CERN, its PS Division and the AD team for building the Antiproton Decelerator – the only facility in the world that is capable of delivering 5.3 MeV antiprotons to us. We profited from the help and personal encouragement of the AD staff, the SPSC, the research directors and the directors general.

This work was supported by the NSF and AFOSR of the US, the BMBF, MPG and FZ-J of Germany, and the NSERC, CRC, CFI and OIT of Canada.

Finally I am grateful to the Harvard University and its physics department for their good natured way of accommodating to a department chair who made weekly trips to CERN to do antihydrogen research, and to the wonderful staff, assistant, research group and family that made it all possible.

XII. References

Adelberger, E.G., and Heckel, B.R. (1991). Adelberger and heckel reply. *Phys. Rev. Lett.* **67**, 1049.

Adelberger, E.G., Heckel, B.R., Stubbs, C.W., and Su, Y. (1991). Does antimatter fall with the same acceleration as ordinary matter? *Phys. Rev. Lett.* **66**, 850–853.

Amoretti, M. *et al.* (2002). Production and detection of cold antihydrogen atoms. *Nature* **419**, 456–459.
Amoretti, M. *et al.* (2003). Positron plasma diagnostics and temperature control for antihydrogen production. *Phys. Rev. Lett.* **91**, 55001.
Amoretti, M. *et al.* (2003). Complete nondestructive diagnostic of nonneutral plasmas based on the detection of electrostatic modes. *Phys. Plas.* **10**, 3056–3064.
Amoretti, M. *et al.* (2004). Dynamics of antiproton cooling in a positron plasma during antihydrogen formation. *Phys. Lett. B* **590**, 133–142.
Amoretti, M. *et al.* (2004). High rate production of antihydrogen. *Phys. Lett. B* **578**, 23–32.
Amoretti, M. *et al.* (2004). The ATHENA antihydrogen apparatus. *Nuc. Inst. Meth. A* **518**, 679–711.
Amoretti, M. *et al.* (2004). Antihydrogen production temperature dependence. *Phys. Lett. B* **583**, 59–67.
Anderegg, F., Hollmann, E.M., and Driscoll, C.F. (1998). Rotating field confinement of pure electron plasmas using trivelpiece-gould modes. *Phys. Rev. Lett.* **81**, 4875–4878.
Armour, E.A.G. (2004a). To be published.
Armour, E.A.G. (2004b). Private communication.
Armour, E.A.G., Chamberlain, C.W. (2001). New Directions in Antimatter Chemistry and Physics. Kluwer Academic, p. 53.
Armour, E.A.G., and Chamberlain, C.W. (2002). Calculation of cross sections for very low-energy hydrogen-antihydrogen scattering using the Kohn variational method. *J. Phys. B* **35**, L489–L494.
Armour, E.A.G., Chamberlain, C.W., Liu, Y., and Martin, G.D.R. (2004). Collisions between low-energy antihydrogen and atoms. *Nuc. Inst. Meth. B* **221**, 1–5.
Aste, A. (1994). Electromagnetic pair production with capture. *Phys. Rev. A* **50**, 3890–3983.
Bass, E.M., and Dubin, D.H.E. (2004). Energy loss rate for guiding-center antihydrogen atoms. *Phys. Plas.* **11**, 1240–1243.
Bates, D.R., Kingston, A.E., and McWhirter, R.W.P. (1962). Recombination between electrons and atomic ions 1. Optically Thin Plasmas. *Proc. Roy. Soc. Lond. A* **267**, 297–312.
Baur, G. (1993). Photon–photon and bremsstrahlung production of fast antihydrogen in $\bar{p}$-nucleus collisions. *Phys. Lett. B* **311**, 343–345.
Baur, G., Boero, G., Brauksiepe, S., Buzzo, A., Eyrich, W., Geyer, R., Grzonka, D., Hauffe, J., Kilian, K., Vetere, M.L., Macri, M., Moosburger, M., Nellen, R., Oelert, W., Passaggio, S., Pozzo, A., Rohrich, K., Sachs, K., Schepers, G., Sefzick, T., Simon, R., Stratmann, R., Stinzing, F., and Wolke, M. (1996). Production of antihydrogen. *Phys. Lett. B* **368**, 251–258.
Bell, J.S. (1987). "Fundamental Symmetries." Plenum, New York, Old and New Theories and Experiments of Gravitation, pp. 1–39.
Bender, C.M., and Orszag, S.A. (1978). "Advanced Mathematical Methods for Scientists and Engineers." McGraw-Hill, New York.
Bertulani, C.A., and Baur, G. (1998). Antihydrogen production and accuracy of the equivalent photon approximation. *Phys. Rev. D* **58**, 34005.
Blanford, G., Christian, D.C., Gollwitzer, K., Mandelkern, M., Munger, C.T., Schultz, J., and Zioulas, G. (1998). Observation of atomic antihydrogen. *Phys. Rev. Lett.* **80**, 3037–3040.
Bluhm, R., Kostelecký, V.A., and Russell, N. (1999). CPT and Lorentz tests in hydrogen and antihydrogen. *Phys. Rev. Lett.* **82**, 2254–2257.
Bollinger, J.J., Heinzen, D.J., Moore, F.L., Itano, W.M., Wineland, D.J., and Dubin, D.H.E. (1993). Electrostatic modes of ion-trap plasmas. *Phys. Rev. A* **48**, 525–545.
Bowden, N.B. (2003). Production of cold antihydrogen during the positron cooling of antiprotons. Ph.D. thesis, Harvard Univ., (thesis advisor: G. Gabrielse).

Brown, L.S., and Gabrielse, G. (1986). Geonium theory: Physics of a single electron or ion in a Penning trap. *Rev. Mod. Phys.* **58**, 233–311.
Cesar, C.L., Fried, D.G., Killian, T.C., Polcyn, A.D., Sandberg, J.C., Yu, I.A., Greytak, T.J., Kleppner, D., and Doyle, J.M. (1996). Two-photon spectroscopy of trapped atomic hydrogen. *Phys. Rev. Lett.* **77**, 255–258.
Chang, Y., and Ordonez, C.A. (2000). Velocity space scattering coefficients with applications in antihydrogen recombination studies. *Phys. Rev. E* **62**, 8564–8572.
Chang, Y., and Ordonez, C.A. (2004). Plasma two-temperature equilibation rate. *Phys. Rev. E* **69**, 037401.
Charlton, M. (1990). Antihydrogen production in collisions of antiprotons with excited states of positronium. *Phys. Lett. A* **143**, 143–146.
Coc, A. *et al.* (1991). Antiproton–proton mass comparison with a radiofrequency mass spectrometer. In: "Low Energy Antiproton Physics – LEAP 90." World Scientific, Singapore, p. 431–436.
Colladay, D., and Kostelecký, V.A. (1997). CPT violation and the standard model. *Phys. Rev. D* **55**, 6760–6774.
Dalgarno, A., Froelich, P., Jonsell, S., Saenz, A., Zygelman, B., 2001. New Directions in Antimatter Chemistry and Physics. Kluwer Academic (Dordrecht), Ch 4. Collisions of H and Hbar, p. 212.
Driscoll, C.F. (2004). Comment on Driven production of cold antihydrogen and the first measured distribution of antihydrogen states. *Phys. Rev. Lett.* **92**, 149303.
Dubin, D.H.E. (2001). Three designs for a magnetic trap that will simultaneously confine neutral atoms and a non-neutral plasma. *Phys. Plas.* **8**, 4331–4339.
Dubin, D.H.E. (1991). Theory of electrostatic fluid modes in a cold spheroidal non-neutral plasma. *Phys. Rev. Lett.* **66**, 2076–2079.
Dubin, D.H.E., and O'Neil, T.M. (1999). Trapped nonneutral plasmas, liquids, and crystals (the thermal equilibrium states). *Rev. Mod. Phys.* **71**, 87–172.
D'Urso, B., Odom, B., Gabrielse, G. (2003). Feedback cooling of a one-electron oscillator. *Phys. Rev. Lett.* **90** (4), 043001.
D'Urso, B., Van Handel, R., Odom, B., Hanneke, D., Gabrielse, G. (2004). Single-particle self-excited oscillator. *Phys. Rev. Lett.* To be published.
Eikema, K.S.E., Walz, J., and Hänsch, T.W. (1999). Continuous wave coherent Lyman-alpha radiation. *Phys. Rev. Lett.* **83**, 3828–3831.
Eikema, K.S.E., Walz, J., and Hänsch, T.W. (2001). Continuous coherent Lyman-α excitation of atomic hydrogen. *Phys. Rev. Lett.* **86**, 5679–5682.
Estrada, J., Roach, T., Tan, J.N., Yesley, P., and Gabrielse, G. (2000). Field ionization of strongly magnetized Rydberg positronium: A new physical mechanism for positron accumulation. *Phys. Rev. Lett.* **84**, 859–862.
Fajans, J., and Schmidt, A. (2004). Malmberg-Penning and Minimum-B trap compatibility: the advantages of higher-order multipole traps. *Nuc. Inst. Meth. A* **521**, 318–325.
Fedichev, P.O. (1997). Formation of antihydrogen atoms in an ultra-cold positron-antiproton plasma. *Phys. Lett. A* **226**, 289–292.
Flannery, M.R., and Vrinceanu, D. (2003). Quantal and classical radiative cascade in Rydberg plasmas. *Phys. Rev. A* **68**, 030502.
Froelich, P. (2002). Quantum chemistry of antimatter. *Adv. Quant. Chem.* **41**, 185–202.
Froelich, P., Jonsell, S., Saenz, A., Eriksson, S., Zygelman, B., and Dalgarno, A. (2004a). Leptonic annihilation in hydrogen-antihydrogen collisions. *Phys. Rev. A* **70**, 022509.
Froelich, P., Jonsell, S., Saenz, A., Zygelman, B., and Dalgarno, A. (2000). Hydrogen anithydrogen collisions. *Phys. Rev. Lett.* **84**, 4577–4580.

Froelich, P., Zygelman, B., Saenz, A., Jonsell, S., Eriksson, S., and Dalgarno, A. (2004b). Hydrogen-antihydrogen molecule and its properties. *Few-Body Syst.* **34**, 63–72.

Fujiwara, M.C. *et al.* (2004). Three-dimensional annihilation imaging of trapped antiprotons. *Phys. Rev. Lett.* **92**, 065005.

Gabrielse, G. (1987). "Penning traps, masses and antiprotons." Bloch, P., Paulopoulos, P., and Klapisch, R. (eds.), "In: Fundamental Symmetries," Plenum, New York, pp. 59–75.

Gabrielse, G. (1988). Trapped antihydrogen for spectroscopy and gravitation studies: Is it possible? *Hyperfine Interact.* **44**, 349–355.

Gabrielse, G. (2001). Comparing the antiproton and proton, and opening the way to cold antihydrogen. *Adv. At. Mol. Opt. Phys.* **45**, 1–39.

Gabrielse, G., 2004. To be published.

Gabrielse, G., Bowden, N.S., Oxley, P., Speck, A., Storry, C.H., Tan, J.N., Wessels, M., Grzonka, D., Oelert, W., Schepers, G., Sefzick, T., Walz, J., Pittner, H., Hänsch, T.W., and Hessels, E.A. (2002a). Background-free observation of cold antihydrogen with field ionization analysis of its excited states. *Phys. Rev. Lett.* **89**, 213401.

Gabrielse, G., Bowden, N.S., Oxley, P., Speck, A., Storry, C.H., Tan, J.N., Wessels, M., Grzonka, D., Oelert, W., Schepers, G., Sefzick, T., Walz, J., Pittner, H., Hänsch, T.W., and Hessels, E.A. (2002b). Driven production of cold antihydrogen and the first measured distribution of antihydrogen states. *Phys. Rev. Lett.* **89**, 233401.

Gabrielse, G., Bowden, N.S., Oxley, P., Speck, A., Storry, C.H., Tan, J.N., Wessels, M., Grzonka, D., Oelert, W., Schepers, G., Sefzick, T., Walz, J., Pittner, H., and Hessels, E.A. (2002c). Stacking of cold antiprotons. *Phys. Lett. B* **548**, 140–145.

Gabrielse, G., Estrada, J., Tan, J.N., Yesley, P., Bowden, N.S., Oxley, P., Roach, T., Storry, C.H., Wessels, M., Tan, J., Grzonka, D., Oelert, W., Schepers, G., Sefzick, T., Breunlich, W., Cargnelli, M., Fuhrmann, H., King, R., Ursin, R., Zmeskal, H., Kalinowsky, H., Wesdorp, C., Walz, J., Eikema, K.S.E., and Hänsch, T. (2001). First positron cooling of antiprotons. *Phys. Lett. B* **507**, 1–6.

Gabrielse, G., *et al.* (2004). ATRAP replies. *Phys. Rev. Lett.* 92, 149304.

Gabrielse, G., Fei, X., Helmerson, K., Rolston, S.L., Tjoelker, R.L., Trainor, T.A., Kalinowsky, H., Haas, J., and Kells, W. (1986b). First capture of antiprotons in a Penning trap: A kiloelectronvolt source. *Phys. Rev. Lett.* **57**, 2504–2507.

Gabrielse, G., Fei, X., Orozco, L.A., Rolston, S.L., Tjoelker, R.L., Trainor, T.A., Haas, J., Kalinowsky, H., and Kells, W. (1989a). Barkas effect observed with antiprotons and protons. *Phys. Rev. A* **40**, 481–484.

Gabrielse, G., Fei, X., Orozco, L.A., Tjoelker, R.L., Haas, J., Kalinowsky, H., Trainor, T.A., and Kells, W. (1989b). Cooling and slowing of trapped antiprotons below 100 meV. *Phys. Rev. Lett.* **63**, 1360–1363.

Gabrielse, G., Fei, X., Orozco, L.A., Tjoelker, R.L., Haas, J., Kalinowsky, H., Trainor, T.A., and Kells, W. (1990). Thousandfold improvement in the measured antiproton mass. *Phys. Rev. Lett.* **65**, 1317–1320.

Gabrielse, G., Haarsma, L., Rolston, S.L. 1989c. Open-endcap Penning traps for high-precision experiments. *Intl. J. Mass Spec. Ion Proc.* **88**, 319–332, ibid. 93, 121 1989.

Gabrielse, G., Hall, D.S., Roach, T., Yesley, P., Khabbaz, A., Estrada, J., Heimann, C., and Kalinowsky, H. (1999a). The ingredients of cold antihydrogen: simultaneous confinement of antiprotons and positrons at 4 K. *Phys. Lett. B* **455**, 311–315.

Gabrielse, G., Khabbaz, A., Hall, D.S., Heimann, C., Kalinowsky, H., and Jhe, W. (1999b). Precision mass spectroscopy of the antiproton and proton using simultaneously trapped particles. *Phys. Rev. Lett.* **82**, 3198–3201.

Gabrielse, G., Rolston, S.L., Haarsma, L., and Kells, W. (1988). Antihydrogren production using trapped plasmas. *Phys. Lett. A* **129**, 38–42.

Gabrielse, G., Speck, A., Storry, C.H., Le Sage, D., Guise, N., Grzonka, D., Oelert, W., Schepers, G., Sefzick, T., Pittner, H., Walz, J., Hänsch, T.W., Comeau, D., Hessels, E.A. (2004a). First evidence for antihydrogen too deeply bound to be guiding center atoms. Submitted for publication.

Gabrielse, G., Speck, A., Storry, C.H., Le Sage, D., Guise, N., Grzonka, D., Oelert, W., Schepers, G., Sefzick, T., Pittner, H., Walz, J., Hänsch, T.W., Comeau, D., and Hessels, E.A. (2004b). First measurement of the velocity of slow antihydrogen atoms. *Phys. Rev. Lett.* **93**, 073401.

Gilson, E., Fajans, J. (1999). Quadrupole induced resonant particle transport in a pure electron plasma. In: "Non-neutral Plasma Physics III." AIP (New York), pp. 250–255.

Gilson, E.P., and Fajans, J. (2003). Quadrupole-induced resonant-particle transport in a pure electron plasma. *Phys. Rev. Lett.* **90**, 015001.

Glinsky, M., O'Neil, T. (1991). Guiding center atoms: Three-body recombination in a strongly magnetized plasma. *Phys. Fluids* **B3**, 1279–1293.

Goldman, T., Hughes, R.J., and Nieto, M.M. (1986). Experimental evidence for quantum gravity? *Phys. Lett. B* **171**, 217–222.

Goldman, T., Nieto, M.M., Holzsheiter, M.H., Darling, T.W., Schauer, M., and Schecker, J. (1991). Comment on "Does antimatter fall with the same acceleration as ordinary matter?" *Phys. Rev. Lett.* **67**, 1048.

Gott, Y.V., Ioffe, M.S., Tel'kovskii, V.G. (1962). Some new results on confinement in magnetic traps. Nuc. Fusion 1962 Suppl. Pt. 3, 1045–1047.

Greaves, R.G., Tinkle, M.D., and Surko, C.M. (1994). Creation and uses of positron plasmas. *Phys. Plas.* **1**, 1439–1446.

Guest, J.R., Choi, J.-H., Raithel, G. (2003). Decay rates of high-$|m|$ Rydberg states in strong magnetic fields. *Phys. Rev. A* **68**, 022509.

Guest, J.R., and Raithel, G. (2003). High-$|m|$ Rydberg states in strong magnetic fields. *Phys. Rev. A* **68**, 052502.

Haarsma, L.H., Abdullah, K., and Gabrielse, G. (1995). Extremely cold positrons accumulated electronically in ultrahigh vacuum. *Phys. Rev. Lett.* **75**, 806–809.

Hall, D.S., and Gabrielse, G. (1996). Electron cooling of protons in a nested Penning trap. *Phys. Rev. Lett.* 77, 1962–1965.

Hess, H.F. (1986). Evaporative cooling of magneticallyl trapped and compressed spin-polarized hydrogen. *Phys. Rev. B* **34**, 3476–3479.

Hess, H.F., Kochanski, G.P., Doyle, J.M., Masuhara, N., Kleppner, D., and Greytak, T.J. (1987). Magnetic trapping of spin-polarized atomic hydrogen. *Phys. Rev. Lett.* **59**, 672–675.

Hessels, E.A., Homan, D.M., and Cavagnero, M.J. (1998). Two-stage Rydberg charge exchange: An efficient method for production of antihydrogen. *Phys. Rev. A* **57**, 1668–1671.

Holzscheiter, M.H., Feng, X., Goldman, T., King, N.S.P., Lewis, R.A., Nieto, M.M., and Smith, G.A. (1996). Are antiprotons forever? *Phys. Lett. A* **214**, 279–284.

Hori, M., Eades, J., Hayano, R.S., Ishikawa, T., Pirkl, W., Widmann, E., Yamaguchi, H., Torii, H.A., Juhász, B., Horváth, D., and Yamazaki, T. (2003). Direct measurement of transition frequencies in isolated $\bar{p}$ He^+ atoms, and new CPT-violation limits on the antiproton charge and mass. *Phys. Rev. Lett.* **91**, 123401.

Hu, S.X., Collins, L.A. (2004). Redistributing populations of Rydberg atoms with half-cycle pulses. *Phys. Rev. A* **69**, 041402(R).

Huang, X.P., Anderegg, F., Hollmann, E.M., Driscoll, C.F., and O'Neil, T.M. (1997). Steady-state confinement of non-neutral plasmas by rotating electric fields. *Phys. Rev. Lett.* **78**, 875–878.

Hughes, R.J., and Deutch, B.I. (1992). Electric charges of positrons and antiprotons. *Phys. Rev. Lett.* **69**, 578–581.

Hughes, R.J., and Holzscheiter, M.H. (1991). Constraints on the gravitational properties of antiprotons and positrons from cyclotron-frequency measurements. *Phys. Rev. Lett.* **66**, 854–857.

Humberston, J.W., Charlton, M., Jacobsen, F.M., and Deutch, B.I. (1987). On antihydrogen formation in collisions of antiprotons with positronium. *J. Phys. B* **20**, L25–L29.

Jelenkovic, B.M., Newbury, A.S., Bollinger, J.J., Itano, W.M., and Mitchell, T.B. (2003). Sympathetically cooled and compressed positron plasma. *Phys. Rev. A* **67**, 063406.

Jonsell, S. (2004). Private communication.

Jonsell, S., Froelich, P., Eriksson, S., Strasburger, K. (2004a). On the strong nuclear force in cold antihydrogen-helium collisions. To be published.Preprint.

Jonsell, S., Saenz, A., Froelich, P. (2000). Low energy hydrogen-antihydrogen collisions. *Nucl. Phys.* **A663&664**, 959c–962c.

Jonsell, S., Saenz, A., Froelich, P., Zygelman, B., and Dalgarno, A. (2001). Stability of hydrogen-antihydrogen mixtures at low energies. *Phys. Rev. A* **64**, 052712.

Jonsell, S., Saenz, A., Froelich, P., Zygelman, B., and Dalgarno, A. (2004b). Hydrogen-antihydrogen scattering in the Born-Oppenheimer approximation. *J. Phys. B* **37**, 1195–1202.

Killian, T.C., Kulin, S., Bergeson, S.D., Orozco, L.A., Orzel, C., and Rolston, S.L. (1999). Creation of an ultracold neutral plasma. *Phys. Rev. Lett.* **83**, 4776–4779.

Killian, T.C., Lim, M.J., Kulin, S., Dumke, R., Bergeson, S.D., and Rolston, S.L. (2001). Formation of Rydberg atoms in an expanding ultracold neutral plasma. *Phys. Rev. Lett.* **86**, 3759–3762.

Kügler, K.-J., Paul, W., and Trinks, U. (1978). A magnetic storage ring for neutrons. *Phys. Lett. B* **72**, 422–424.

Kuzmin, S.G., O'Neil, T.M., Glinsky, M.E. (2004a). Guiding center drift atoms. *Phys. Plas.* **11**(5), 2382–2393.

Kuzmin, S.G., O'Neil, T.M. (2004b). Motion of guiding center drift atoms in the electric and magnetic fields of a Penning trap. Preprint.

Kuzmin, S.G., O'Neil, T.M. (2004c). Polarization and trapping of weakly bound atoms in Penning trap fields. *Phys. Rev. Lett.* **92**, 243401.

Lehnert, B. (1964). "Dynamics of Charged Particles." Wiley, New York.

Makin, B., and Keck, J.C. (1963). Variational theory of three-body electron-ion recombination rates. *Phys. Rev. Lett.* **11**, 281–283.

Men'shikov, L.I., Fedichev, P.O. (1995). Theory of elementary atomic processes in an ultracold plasma. *Zh. Éksp. Teor. Fiz.* **108**, 144–162, jETP 81, 78–86.

Merrison, J.P., Bluhme, H., Chevallier, J., Deutch, B.I., Hvelplund, P., Jørgensen, L.V., Knudsen, H., Poulsen, M.R., and Charlton, M. (1997). Hydrogen formation by proton impact on positronium. *Phys. Rev. Lett.* **78**, 2728–2731.

Migdall, A.L., Prodan, J.V., Phillips, W.D., Bergeman, T.H., and Metcalf, H.J. (1985). First observation of magnetically trapped neutral atoms. *Phys. Rev. Lett.* **54**, 2596–2599.

Mohri, A., and Yamazaki, Y. (2003). A possible new scheme to synthesize antihydrogen and to prepare a polarized antihydrogen beam. *Europhys. Lett.* **63**, 207–213.

Morpurgo, G. (1991). Adelberger, E.G.; and Heckel, B.R. Comment on "Does antimatter fall with the same acceleration as ordinary matter?" *Phys. Rev. Lett.* **67**, 1047.

Munger, C.T., Brodsky, S.J., and Schmidt, I. (1993). Production of relativistic antihydrogen atoms by pair production with positron capture and measurement of the Lamb shift. *Hyperfine Interact.* **76**, 175–180.

Munger, C.T., Brodsky, S.J., and Schmidt, I. (1994). Production of relativistic antihydrogen atoms by pair production with positron capture. *Phys. Rev. D* **49**, 3228–3235.

Niering, M., Holzwarth, R., Reichert, J., Pokasov, P., Udem, T., Weitz, M., Hänsch, T.W., Lemonde, P., Santarelli, G., Abgrall, M., Laurent, P., Salomon, C., and Clairon, A. (2000). Measurement of the hydrogen 1s–2s transition frequency by phase coherent comparison with a microwave cesium fountain clock. *Phys. Rev. Lett.* **84**, 5496–5499.

Nieto, M.M., and Goldman, T. (1991). The arguments against "antigravity" and the gravitational acceleration of antimatter. *Phys. Rep.* **205**, 221–281.

O'Neil, T.M. (1980). A confinement theorem for nonneutral plasmas. *Phys. Fluids* **23**, 2216–2218.

Ordonez, C.A. (1997). Confinement of a neutral plasma using nested electric potential wells. *Phys. Plas.* **4**, 2313–2315.

Ordonez, C.A., Dolliver, D.D., Chang, Y., and Correa, J.R. (2002). Possibilities for achieving antihydrogen recombination and trapping using a nested Penning trap and a magnetic well. *Phys. Plas.* **9**, 3289–3302.

Oshima, N., Kojima, T.M., Niigaki, M., Mohri, A., Komaki, K., Iwai, Y., and Yamazaki, Y. (2003). Development of a cold HCI source for ultra-slow collisions. *Nuc. Inst. Meth. B* **205**, 178–182.

Oxley, P., Bowden, N.S., Parrott, R., Speck, A., Storry, C., Tan, J.N., Wessels, M., Gabrielse, G., Grzonka, D., Oelert, W., Schepers, G., Sefzick, T., Walz, J., Pittner, H., Hänsch, T.W., Hessels, E.A. (August 2004). Aperture method to determine the density and geometry of antiparticle plasmas. *Phys. Lett. B* **595**, 60–67.

Peil, S., and Gabrielse, G. (1999). Observing the quantum limit of an electron cyclotron: QND measurements of quantum jumps between fock states. *Phys. Rev. Lett.* **83**, 1287–1290.

Pritchard, D.E. (1983). Cooling neutral atoms in a magnetic trap for precision spectroscopy. *Phys. Rev. Lett.* **51**, 1336–1339.

Roberts, J.L., Fertig, C.D., Lim, M.J., Rolston, S.L. (2004). Electron temperature of ultracold plasmas. *Phys. Rev. Lett.* **92**, 253003.

Robicheaux, F. (2004). Simulation of antihydrogen formation. *Phys. Rev. A* **70**, 022510.

Robicheaux, F., and Hanson, J.D. (2004). Three-body recombination for protons moving in a strong magnetic field. *Phys. Rev. A* **69**, 010701.

van Roijen, R., Berkhout, J.J., Jaakola, S., and Walraven, J.T.M. (1988). Experiments with atomic hydrogen in a magnetic trapping field. *Phys. Rev. Lett.* **61**, 931–934.

Schwinberg, P.B., R.S. Van Dyck, Jr., and Dehmelt, H.G. (1981). Trapping and thermalization of positrons for geonium spectroscopy. *Phys. Lett. A* **81**, 119–120.

Setija, I.D., Werij, H.G.C., Luiten, O.J., Reynolds, M.W., Hijmans, T.W., and Walraven, J.T.M. (1993). Optical cooling of atomic hydrogen in a magnetic trap. *Phys. Rev. Lett.* **70**, 2257–2260.

Shlyapnikov, G.V., Walraven, J.T.M., E.L. Surkov (1993). Antihydron at sub-Kelvin temperatures, *Hyperfine Interact.* **76**, 31–46.

Simien, C.E., Chen, Y.C., Gupta, P., Laha, S., Martinez, Y.N., Mickelson, P.G. Nagel, S.B., and Killian, T.C. (2004). Using absorption imaging to study ion dynamics in an ultracold neutral plasma. *Phys. Rev. Lett.* **92**, 143001.

Sinha, P.K., and Ghosh, A.S. (2003). Ultracold elastic bar-He scattering. *Phys. Rev. A* **68**, 022504.

Speck, A., Storry, C.H., Hessels, E., and Gabrielse, G. (2004). Laser-controlled production of Rydberg positronium via charge exchange collisions. *Phys. Lett. B* **597**, 257–262.

Squires, T.M., Yesley, P., and Gabrielse, G. (2001). Stability of a charged particle in a combined Penning-Ioffe trap. *Phys. Rev. Lett.* **86**, 5266–5269.

Stevefelt, J., Boulmer, J., and Delpech, J.F. (1975). Collisional-radiative recombination in cold plasmas. *Phys. Rev. A* **12**, 1246–1251.

Storry, C.H., Speck, A., Le Sage, D., Guise, N., Gabrielse, G., Grzonka, D., Oelert, W., Schepers, G., Sefzick, T., Walz, J., Pittner, H., Herrmann, M., Hänsch, T.W., Comeau, D., Hessels, E.A. (2004). First laser-controlled antihdyrogen production. *Phys. Rev. Lett.* **93**, 263401.

Strasburger, K., and Chojnacki, H. (2002). Helium-antihydrogen interaction: The Born-Oppenheimer potential energy curve. *Phys. Rev. Lett.* **88**, 163201.

Surko, C.M., Greaves, R.G., and Charlton, M. (1997). Stored positrons for antihydrogen production. *Hyperfine Interact.* **109**, 181–188.

Thompson, J.K., Rainville, S., and Pritchard, D.E. (2004). Cyclotron frequency shifts arising from polarization forces. *Nature* **430**, 58–61.

Tinkle, M.D., Greaves, R.G., and Surko, C.M. (1996). Modes of spheroidal ion plasmas at the Brillouin limit. *Phys. Plas.* **3**, 749–758.

Todd *et al.*, A., 2004. To be published.

VanDyck, R.S.Jr., Schwinberg, P.B., and Dehmelt, H.G. (1987). New high-precision comparison of electron and positron g-factors. *Phys. Rev. Lett.* **59**, 26–29.

Verdú, J., Beier, T., Djekić, S., Häffner, H., Kluge, H.-J., Quint, W., Valenzuela, T., Vogel, M., and Werth, G. (2003). The magnetic moment anomaly of the electron bound in hydrogen-like oxygen $^{16}O^{7+}$. *J. Phys. B* **36**, 655–663.

Voronin, A.Y., and Carbonell, J. (2004). Hydrogen-antyhydrogen atomic interaction at subkelvin temperatures. *Nuc. Inst. Meth. B* **214**, 139–143.

Vrinceanu, D., Granger, B.E., Parrott, R., Sadeghpour, H.R., Cederbaum, L., Mody, A., Tan, J., and Gabrielse, G. (2004). Strongly magnetized antihydrogen and its field ionization. *Phys. Rev. Lett.* **92**, 133402.

Walz, J., and Hänsch, T. (2004). A proposal to measure antimatter gravity using ultracold antihydrogen atoms. *General Relativity and Gravitation* **36**, 561–570.

Weimer, C.S., Bollinger, J.J., Moore, F.L., and Wineland, D.J. (1994). Electrostatic modes as a diagnostic in Penning-trap experiments. *Phys. Rev. A* **49**, 3842–3853.

Wesdorp, C., Robicheaux, F., and Noordam, L.D. (2000). Field-induced electron-ion recombination: A novel route towards neutral (anti-)matter. *Phys. Rev. Lett.* **84**, 3799–3802.

Wineland, D.J., Weimer, C.S., and Bollinger, J.J. (1993). Laser-cooled positron source. *Hyperfine Interact.* **76**, 115–125.

Wolf, A. (1993). Laser-stimulated formation and stabilization of antihydrogen atoms. *Hyperfine Interact.* **76**, 189–201.

Yamazaki, T. *et al.* (2004). To be published.

Zimmerman, C., and Hänsch, T. (1993). Laser spectroscopy of hydrogen and antihydrogen. *Hyperfine Interact.* **76**, 47–57.

Zygelman, B. Recombination of antiprotons with positrons at low temperatures. *J. Phys. B* **36**, L31–L37.

Zygelman, B., Dalgarno, A., 1989. (private communication).

Zygelman, B., Saenz, A., Froelich, P., and Jonsell, S. (2004). Cold collisions of atomic hydrogen with antihydrogen atoms: An optical potential approach. *Phys. Rev. A* **69**, 042715.

Zygelman, B., Saenz, A., Froelich, P., Jonsell, S., and Dalgarno, A. (2001). Radiative association of atomic hydrogen with antihydrogen at subkelvin temperatures. *Phys. Rev. A* **63**, 052722.